Geophys. J. Int. (2001) **145,** 349–367

Three-dimensional flexural modelling of the Ebro Basin (NE Iberia)

J. M. Gaspar-Escribano,[1] J. D. van Wees,[1] M. ter Voorde,[1] S. Cloetingh,[1] E. Roca,[2] L. Cabrera,[2] J. A. Muñoz,[2] P. A. Ziegler[3] and D. Garcia-Castellanos[1],

[1] *Faculteit der Aardwetenschappen, Vrije Universiteit, De Boelelaan* 1085, 1081 *HV Amsterdam, The Netherlands. E-mail: gasj@geo.vu.nl*
[2] *Facultat de Geologia, Universitat de Barcelona, c/Martí Franqués s/n,* 08071 *Barcelona, Spain*
[3] *Geological-Palaeontological Institute, University of Basel, Bernoullistrasse* 32, 4065 *Basel, Switzerland*

Accepted 2000 November 18. Received 2000 November 1; in original form 2000 January 6

SUMMARY

The Ebro Basin, the southern foreland basin of the Pyrenees, has undergone a complex evolution in which, apart from the Pyrenees, the Iberian Range and the Catalan Coastal Ranges have played an important role, both as sediment sources and as basin confining structures. The deflected basement underlying the Ebro Basin dips north, suggesting a lithospheric-scale control on the structure of this basin. This is compatible with the results of subsidence analyses, which show that the study area is not in a local mode of isostatic compensation.

In order better to understand the mechanisms that led to the present configuration of the Ebro Basin, and particularly the relevance of the various kinds of (un)loading (e.g. surrounding fold-and-thrust belts, basin topography, subsurface loads), we carried out a 3-D kinematic modelling study that accounts for the flexural state of the lithosphere, subjected to various loads applied at its lateral boundaries, and the sedimentary fill of the basin. We also included the effect of Neogene extensional tectonics along the eastern basin margin, which is related to the opening of the Valencia Trough.

We show the suitability of the 3-D lithospheric-scale flexural modelling approach to the study of NE Iberia. Modelling results point to a relatively strong lithosphere in this area, with values of effective elastic thickness ranging from 10 to 35 km in the Ebro Basin, increasing towards the Pyrenees. We also find that the topographic (tectonic) load itself is insufficient to explain the observed basement deflection. Thus an extra subsurface load beneath the Pyrenees, corresponding to the underthrusted Iberian lithosphere, is required. The effect of lithospheric stretching in the Valencia Trough on the Ebro Basin is appreciable only in its eastern part, where the lithosphere was uplifted. This had considerable repercussions on the sedimentary and erosional regime of the Ebro Basin. We have analysed the link between the stretching-related, tectonically uplifted areas and the erosional patterns observed onshore northeast Iberia.

Key words: 3-D numerical modelling, Ebro Basin, erosion, flexure, subsidence, surface processes, Valencia Trough.

1 INTRODUCTION

The northeastern region of the Iberian Peninsula (Fig. 1) is located in an area that, since the end of the Variscan orogeny, has undergone several stages of deformation involving mechanisms such as extension, compression, or even both simultaneously (Vegas & Banda 1982; Roca & Guimerà 1992; Salas & Casas 1993; Vergés & García-Senz, 2000). The resultant structural–geomorphological setting reflects the complexities of the polyphase evolution of this area.

The late Mesozoic–Cenozoic convergence of the African and Eurasian plates led to the collision of the Iberian and the European plates and the development of the Pyrenean orogen, which is characterized by a considerably thickened upper crust (Muñoz 1992). The Iberian Range and the Catalan Coastal Ranges developed in the interior of the Iberian plate in response to compressional deformation of Mesozoic rifted basins (Vegas & Banda 1982). The location of these three fold-and-thrust belts was controlled by pre-existing crustal weakness zones, provided by Mesozoic extensional fault systems

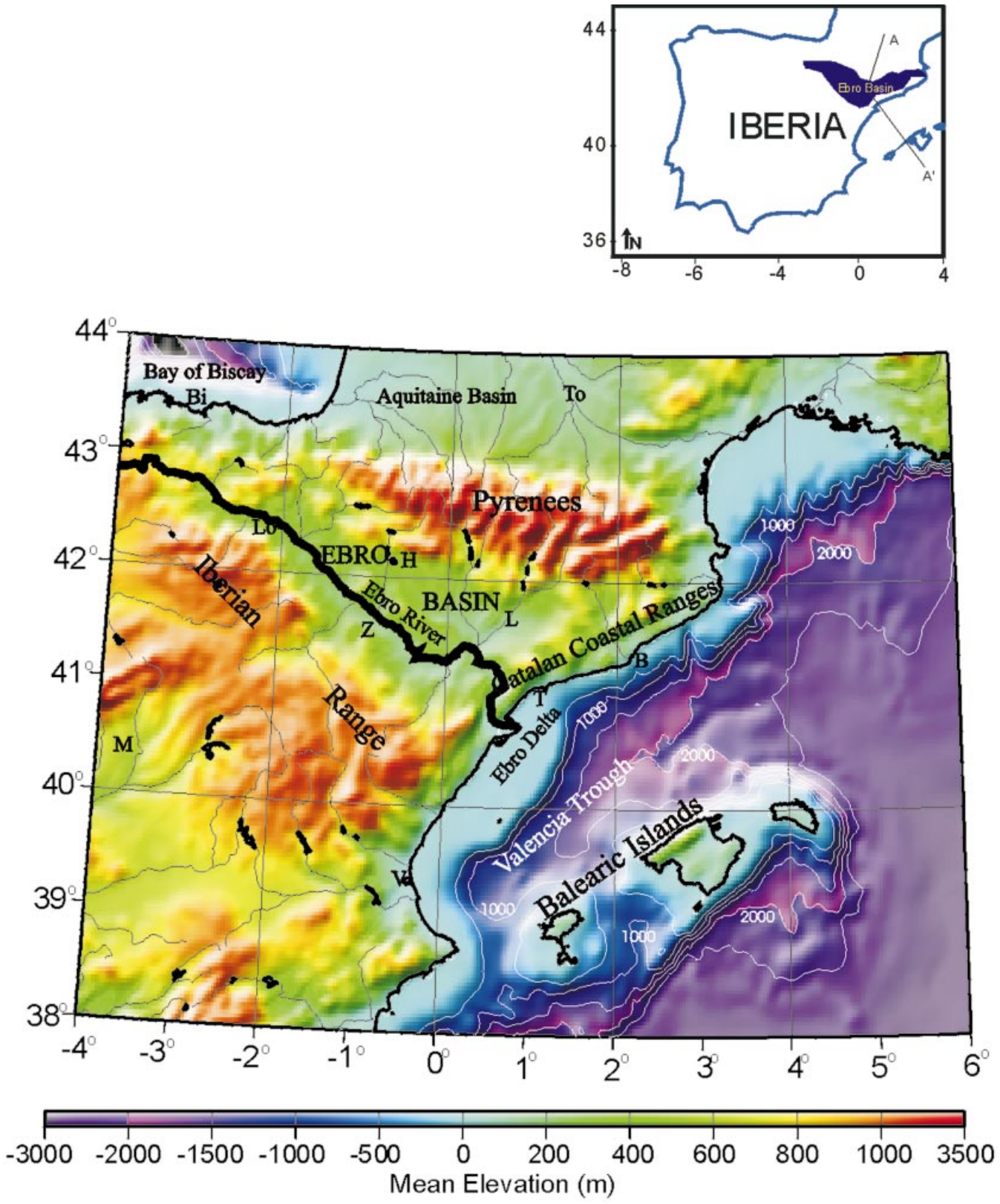

Figure 1. Topographic and bathymetric map of northeastern Iberia and the northwestern Mediterranean, including the main rivers. The Ebro River is highlighted. Note the large prograding shelf-talud of the Ebro Delta. The contour interval of bathymetry is 500 m. B: Barcelona, Bi: Bilbao, H: Huesca, L: Lleida, Lo: Logroño, M: Madrid, T: Tarragona, To: Toulouse, V: Valencia, Z: Zaragoza. Line A–A′ refers to Fig. 2.

(Roca & Guimerà 1992; Van Wees & Stephenson 1995; Beaumont *et al*. 2000). Since Late Oligocene–Early Miocene times, the eastern part of the Iberian plate has been affected by the extensional tectonics related to the opening of the northwestern Mediterranean Basin (Roca 2000). Both the crust and the lithospheric mantle are thinned beneath the Valencia Trough (Torné *et al*. 1996), although the extent to the Iberian inland, where this rifting stage deformed the lithosphere, is not well constrained. The Ebro Basin is surrounded by the Pyrenees, the Iberian and the Catalan Coastal ranges, and records the tectonic events controlling their evolution. Therefore its study can constrain the interrelationships between these events.

The configuration of the basement underlying the Cenozoic Ebro Basin, mainly northward-dipping, indicates that the Pyrenees exerted a large-scale control on the lithospheric flexure of their foreland. There are, however, a number of observations that suggest that other mechanisms contributed to the development of the Ebro Basin, thus necessitating an analysis of its 3-D (or even 4-D, if temporal evolution is included) setting (Figs 1 and 3):

(1) the Ebro Basin presents an asymmetrical triangular shape;

(2) the basement of the Ebro Basin is not uniformly deflected, neither in direction nor magnitude of plate bending, in front of the surrounding fold-and-thrust belts (Pyrenees, Iberian and Catalan Coastal ranges);

(3) During the development of the Ebro Basin, the controlling stress field underwent a complex evolution (Guimerà 1984), including phases of N–S compression during the Eocene and Oligocene, and NW–SE extension during the Late Oligocene–Early Miocene development of the Valencia Trough;

(4) During Plio-Miocene times, the northeasternmost part of the Ebro basin was uplifted and tilted westwards.

As the stratigraphic and structural record of the Ebro Basin and its surrounding fold-and-thrust belts is remarkably well exposed in outcrops, and supplemented by a wealth of data coming from a variety of sources (e.g. well data, seismic sections), this area is particularly well suited for studying the evolution of foreland basins, and specifically basin flexural behaviour.

In view of this, many authors have designed flexural modelling studies in the Ebro Basin. Brunet (1986) modelled a section across the conjugate foreland basins of the Pyrenees (the Aquitaine Basin to the north and Ebro Basin to the south), including sedimentary load and varying the flexural rigidity of the lithosphere beneath the orogen. She considered a broken plate model with vertical shear forces at the boundary, thought to be related to the subducted cold lithospheric root of the Pyrenees. Desegaulx & Moretti (1988) also modelled the flexure of the lithosphere subjected to surface loads and concluded that the northwestern Iberian Range thrust front significantly influenced the basin geometry. Zoetemeijer *et al*. (1990) studied the flexural response of the lithosphere to topographic and subsurface loads along three profiles through the Ebro Basin, constraining their model with gravity and well data, and relating their results to observed heat flow patterns. To obtain a good fit they had to vary laterally the effective elastic thickness (T_e) of the lithosphere, and, except for the westernmost profile (Navarra–Rioja zone), concluded that subsurface loads could be neglected. Desegaulx *et al*. (1990) analysed the flexural history of the Iberian and European plates, constraining their model with backstripping results and gravity data, and assuming a constant T_e and no subsurface loads. They concluded that the European plate is less rigid than the Iberian plate as a result their different stretching histories, primarily the Late Jurassic–Early Cretaceous crustal extension that weakened the European plate to a higher degree (see also Desegaulx *et al*. 1991). Millán *et al*. (1995) carried out flexural modelling of the lithosphere using gravity data, incorporating subsurface loads, spatial and temporal variations of T_e, and the effects of palaeotopographic variations in the external parts of the Pyrenees. Their results suggest that the pre-orogenic Cretaceous extensional phase had only a minor effect on the actual flexural rigidity of the lithosphere. Finally, Waltham *et al*. (2000), analysed the subsidence history of a small part of the Ebro Basin using a flexural model, and concluded that the lithosphere as a whole is flexed down in response to its tectonic loading and that the crust is detached from the mantle lithosphere at lower crustal levels, the upper crust being subjected to stress-induced buckling (see also Cloetingh *et al*. 1999).

Although many authors have addressed the flexural behaviour of the Ebro Basin, their hypotheses differ widely and sometimes oppose each other. Most of the studies were carried out along cross-sections, ignoring or neglecting the effects of processes acting out of the plane of section. Only Desegaulx & Moretti (1988) carried out a 3-D analysis. Their model, however, was limited in a number of ways, namely by (1) not considering regional variations in lithospheric strength; (2) not addressing the effects of the topographic load of the Catalan Coastal Ranges and the extension in the Valencia Trough; and (3) not including the topography of the whole study area in their loading calculations. This means that they neglect a topographic load that in some cases reaches altitudes of 500–1000 m, which must have an important effect.

The objective of this paper is to study the flexural behaviour of the lithosphere in northeastern Iberia and to establish which assumptions are the most plausible in a first-order approach. For this purpose, we carried out a 3-D numerical modelling study, covering the entire area addressed, and investigated the role that various types of loads (e.g. topographic/tectonic loads, subsurface loads, etc.) play in the system, constraining the amplitude and extent of the resulting deformations. Furthermore, we investigated the effects of other events on the Ebro Basin that traditionally are considered of second-order relevance, such as the Neogene extensional tectonics in the Valencia Trough.

2 GEOLOGICAL SETTING AND TEMPORAL EVOLUTION

The evolution of the Cenozoic Ebro Basin was influenced and controlled by the development of the thrust-and-fold belts that surround it, as well as by the opening of the Valencia Trough. In this section we describe these structural units and review the temporal evolution of NE Iberia, stressing the interplay of the individual processes that led to the actual configuration of the Ebro Basin. The differences between long- and short-wavelength phenomena and their relative relevance will be highlighted.

2.1 Morphotectonics

The Ebro Basin and its surrounding structural units have distinct topographical expressions. The main morpho-tectonic features of each structural unit are depicted in Figs 1, 2 and 5(b), and briefly described below:

The *Pyrenees* are a continent–continent collisional double-wedged, asymmetrical orogen that strikes E–W. The southern orogenic wedge is more developed than the northern one (Figs 1 and 2). The central (or axial) part of the chain consists of an antiformal stack of Palaeozoic basement imbrications with a maximum structural relief of 20 km, as estimated from restored crustal cross-sections (Muñoz 1992; Teixell 1998). The external part of the south Pyrenean wedge involves Triassic to Late Cretaceous syn-and post-rift sediments and Senonian–Early Miocene syn-orogenic sediments deposited in piggy-back basins as well as in the foreland basin. The end of the deformation migrated along-strike westwards, from the Middle Oligocene in the eastern Pyrenees to the Middle Miocene in the western Pyrenees (Vergés *et al*. 1995). In contrast to the rest of the mountain chain, no underthrusting is identified in the westernmost Pyrenees (Souriau & Granet 1995; Ledo *et al*. 2000). The total amount of shortening is higher in the eastern and central areas (about 150–175 km, Muñoz 1992; Beaumont *et al*. 2000) than in the western Pyrenees (80 km, Teixell 1998). Deep structure studies of the Pyrenees show that the under-thrusted Iberian lithosphere reaches depths of 80–100 km (Souriau & Granet 1995; Pous *et al*. 1995a,b; Ledo *et al*. 2000).

The *Iberian Range* consists of folded and thrusted Palaeozoic and Mesozoic–Cenozoic rocks, cropping out along NW–SE-trending structures (Fig. 1), that resulted from the inversion of Mesozoic extensional basins (Salas & Casas 1993; Van Wees *et al*. 1998; Salas *et al*. 2000). Inversion movement commenced during the Late Eocene?–Oligocene (Guimerà 1994), at a time when the older Pyrenean thrust sequences were already formed, and continued until Miocene times. The age of the youngest Iberian structures is Early Miocene in the east and Middle Miocene towards the west. The development of this intraplate fold-and-thrust belt involved a total shortening of about 75 km with a maximum crustal thickening of 11 km (Guimerà *et al*. 1996).

The *Catalan Coastal Ranges* are the frontal part of a NE–SW-striking, inverted Early Mesozoic extensional basin, part of which is hidden beneath the Valencia Trough (Fig. 1). The structural style is mostly dominated by basement-involving steep upthrusts that reactivated Mesozoic extensional faults (Figs 2b, 5b). Crustal shortening and thickening are limited to 10–12 km and 2 km, respectively (Lawton *et al*. 1999). The age of the contractional structures ranges from Middle Eocene to Late Oligocene (Anadón *et al*. 1985).

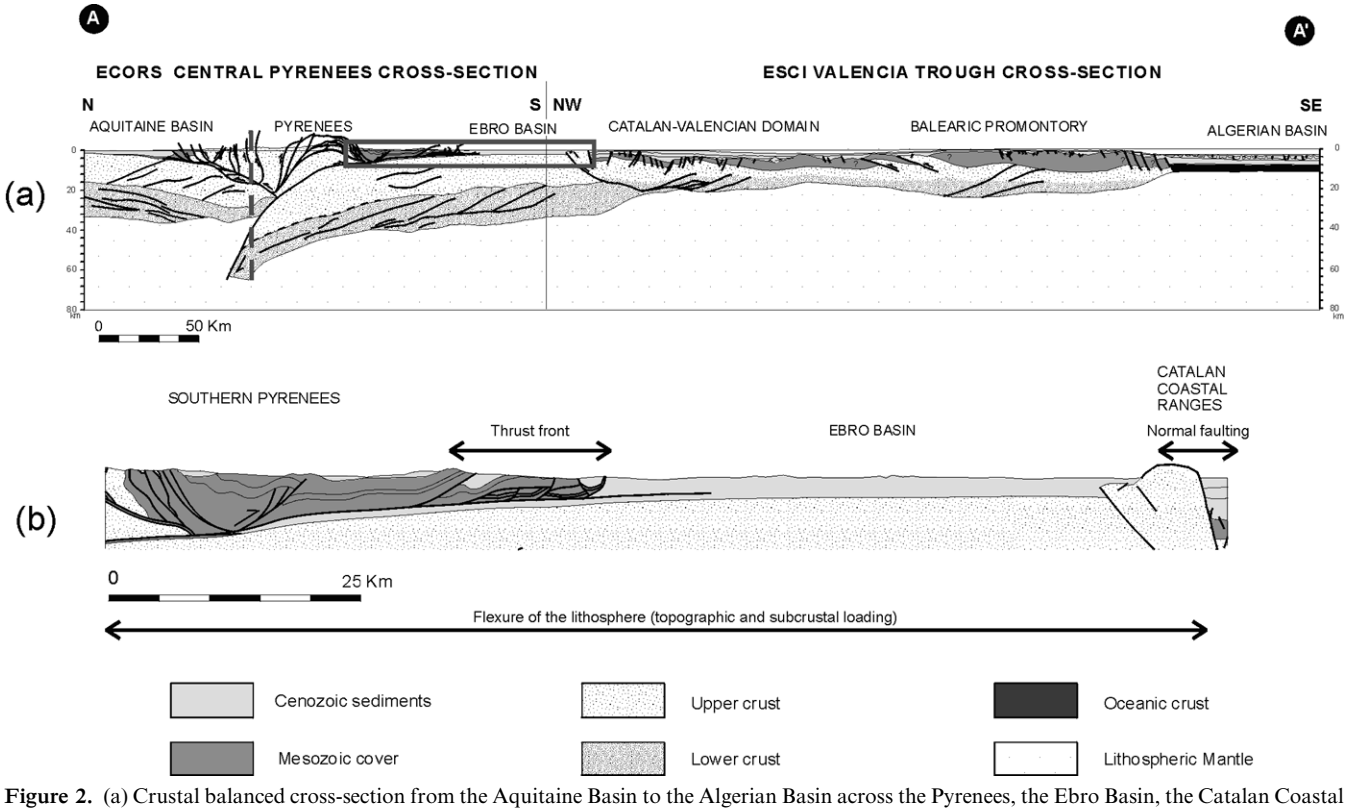

Figure 2. (a) Crustal balanced cross-section from the Aquitaine Basin to the Algerian Basin across the Pyrenees, the Ebro Basin, the Catalan Coastal Ranges and the Valencia Trough. The Pyrenees cross-section is from Beaumont *et al*. (2000), and the Valencia Trough cross-section from Sàbat *et al*. (1997). The vertical dashed line indicates the approximate location of the assumed free, broken plate boundary (see Section 4 for explanation). **(b)** Zoom of the Ebro Basin and surroundings (framed area in part a) showing the different wavelengths of the tectonic processes involved in the configuration of the region. The long arrow indicates long-wavelength processes associated with lithospheric flexure arising from topographic/tectonic loads and subcrustal loads. Short arrows show short-wavelength phenomena, such as those produced by the entrapment of low-density bodies beneath the south Pyrenean thrust front and those related to the Catalan Coastal Ranges normal fault system. The approximate location of the cross-section is shown in Fig. 1.

The *Ebro Basin* is underlain by a 32 km thick crust that has been at best only slightly deformed since the Variscan orogeny (Figs 1 and 2). The fill of this basin consists of autochthonous flat-lying Palaeogene and Early Neogene sediments which extend beneath the thrusts of the Pyrenees and the western Iberian Range as far as 40 and 28 km, respectively (Berástegui *et al.* 1993; Salas *et al.* 2000). The thickest successions are preserved close to the deformation front of the Pyrenees, attaining 4000 m in the western parts of the Ebro Basin. The age of the rocks underlying the Tertiary Ebro Basin infill is Palaeozoic and Permo-Triassic in the east, Jurassic in the centre of the basin and Permo-Triassic to the west, with Cretaceous sparsely found. The age of the youngest preserved sediments is Late Eocene in the eastern part of the Ebro Basin and Late Miocene in the western parts (Riba *et al.* 1983). This results from the non-deposition or erosion of thin Neogene sediments in the eastern Ebro Basin and a westward decreasing amount of erosion (Anadón *et al.* 1989).

The *Valencia Trough* (Figs 1 and 2) is a Late Oligocene–Neogene extensional basin that is superimposed on the inverted Mesozoic basins of the Iberian and Catalan Coastal ranges (Roca & Desegaulx 1992). The major basin-bounding extensional faults of the Valencia Trough are located close to the Mediterranean coast, either offshore or onshore, where they reactivate the main (Palaeogene) contractional faults of the Catalan Coastal Ranges (Anadón *et al.* 1985) (Figs 2b, 5b). Compressional tectonics related to the development of the Betic deformational front affected the southeastern margin of the basin (Roca & Desegaulx 1992). In the centre of the basin the crust has been substantially thinned, crustal thicknesses reaching values as low as 8 km (Sàbat *et al.* 1997). The basin fill consists of a 2–3 km thick succession of Late Oligocene–Quaternary sediments unconformably overlying a fairly continuous, well-developed Palaeozoic–Mesozoic substratum (Clavell & Berástegui 1991; Bartrina *et al.* 1992). Two depositional megasequences are recognized (Roca *et al.* 1999): (1) the lower one is composed of Late Oligocene–Early Miocene syn-rift clastics and carbonates, mostly restricted to the grabens; (2) the upper one, Middle Miocene–Quaternary in age, was deposited during the post-rift stage and deeply buries the grabens and their flanks. Depositional evolution of this second megasequence is characterized by an initial progressive restriction of carbonate sedimentation, followed by the development of thick progradational shelf-slope terrigenous systems that record both the availability of large accommodation space and an increasing clastic supply from the Ebro Basin and surrounding orogens, commencing in Serravalian times (Bartrina *et al.* 1992; Roca & Desegaulx 1992).

2.2 Geological evolution

During Mesozoic times, Iberia was submitted to an extensional stress field related to the opening of the Atlantic and Tethys oceans and the Bay of Biscay (Ziegler 1988; Roest & Srivastava 1991). Major sedimentary basins developed along the margins of the area that presently is occupied by the Ebro Basin, which remained as a rather stable block during most of the Mesozoic.

During the Late Cretaceous, the stress field changed in response to the onset of the N–S convergence of Africa and Eurasia. In NE Iberia deformation was initially localized in the area of the future Pyrenees, which were the first fold-and-thrust belt to grow. At this stage, foreland basin sedimentation was restricted to narrow and strongly subsiding troughs in front of the inverting Early Cretaceous extensional basins (Vergés & García-Senz, 2000). At this time, the southward adjacent area of the Ebro Basin was uplifted, and then emerged and subjected to erosion (Puigdefàbregas & Souquet 1986).

During the Palaeocene–Eocene, deposition of marine and continental sediments transgressed on the basal Tertiary unconformity of the evolving Ebro foreland basin, with the basin margin progressing southwards ahead of the south Pyrenean thrust sheets. The progressive southward advance of the thrust front resulted in the incorporation of foreland basin series into the Pyrenees, as well as the development of piggy-back basins (Puigdefàbregas *et al.* 1986). Eocene foreland basin sediments occupied a wide area that extended a considerable distance southwards and eastwards of the present Ebro Basin limits (Fig. 3). This reflects the fact that during this period the lithosphere responded by long-wavelength deflection to the loads exerted on it by the Pyrenees. Initial uplift pulses are Early–Middle Eocene in the Catalan Coastal Ranges (Anadón *et al.* 1985) and probably not younger in the Iberian Range (Late Eocene?–Oligocene, Guimerà 1984, 1994).

During the Late Eocene, the progressive uplift of the western Pyrenees resulted in the closure of connections between the Ebro foreland basin and the Atlantic Ocean, implying the end of marine sedimentation. At the same time, inversion and uplift of the Iberian and Catalan Coastal ranges closed off the Ebro Basin to the SW and SE, which thus became tectonically silled. In conjunction with the progressive (basin-wards) development of the surrounding fold-and-thrust belts, more significant on the Pyrenean boundary than on any other (Fig. 2b), the area of the Ebro Basin became smaller. Moreover, the erosional base level of this now tectonically silled basin gradually rose, with detritus derived from its bounding ranges infilling the newly created accommodation space. This is particularly evident in the burial of the South Pyrenean thrust sheets by 2–3 km of their own debris (Coney *et al.* 1996; Fitzgerald *et al.* 1999).

The next cycle in the basin history began during the Late Oligocene, with the onset of rifting in the Valencia Trough (Fig. 3). This had a number of important consequences for the eastern part of the study region, namely: (1) progressive erosion of the Iberian and Catalan Coastal ranges; (2) the development of new accommodation space in the area of the rapidly subsiding Valencia Trough; and (3) lithospheric uplift of the Catalan Coastal Ranges area (rift shoulder effect).

Since the beginning of the Palaeocene, the Ebro Basin has been the site of sediment accumulation, first of both marine and non-marine and later of only continental sediments. After the Late Eocene, discharge from the Ebro Basin to adjacent areas was interrupted, due to its tectonic silling. Hence during the Late Oligocene–Early Miocene the basin surface must have been located significantly above sea level. Correspondingly, its sedimentary fill must have exerted an important loading effect on the lithosphere, affecting the whole region. This process continued until the Middle Miocene, by which time the Ebro River had cut through the Catalan Coastal Ranges and progressively captured its present headwaters during the Late Miocene. From Middle Miocene times onwards, the sedimentary fill of the Ebro Basin was progressively eroded, with the Ebro River discharging erosion products into the Valencia Trough. Correspondingly, the lithosphere of the entire Ebro Basin was erosionally unloaded and uplifted during Late Miocene and more recent times (Vergés *et al.* 1998; Fitzgerald *et al.* 1999).

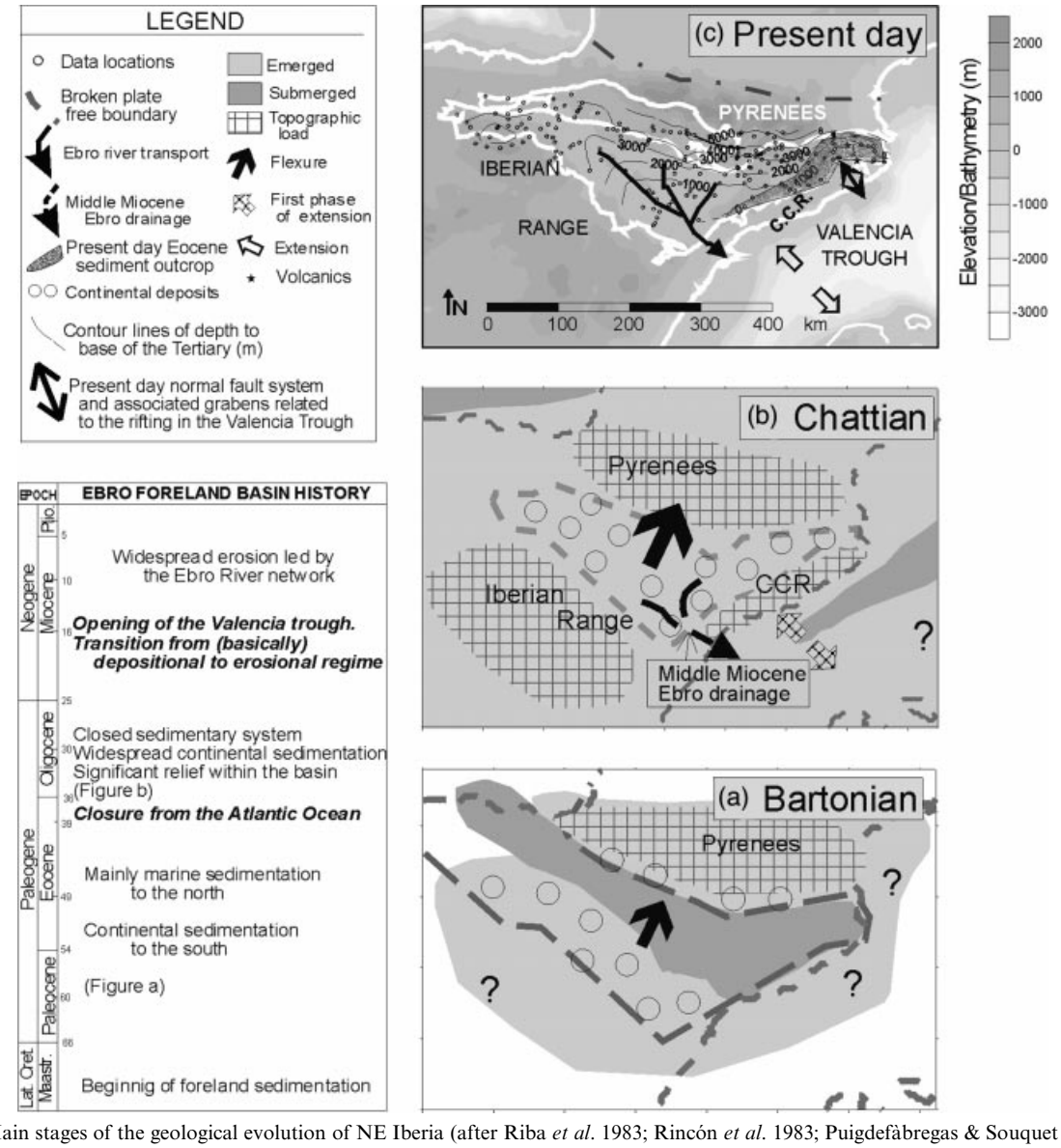

Figure 3. Main stages of the geological evolution of NE Iberia (after Riba *et al*. 1983; Rincón *et al*. 1983; Puigdefàbregas & Souquet 1986; Muñoz 1992; Roca & Guimerà 1992; Salas & Casas 1993 and Coney *et al*. 1996). (a) Bartonian (Late Eocene): initial marine transgression. The northern part of the basin is submerged, whilst the southern part records continental sedimentation. The topography is not very developed, except in the Pyrenees. It is the final phase of marine sedimentation in the basin. (b) Chattian (Late Oligocene): the effect of the tectonic–topographic loads (mainly the Pyrenees) is important all over the basin, flexing down the lithosphere to the north. Coeval with regional N–S compression, rifting in the Valencia Trough implies an onset of NW–SE extension. During the Oligocene and Early Miocene, the Ebro Basin is closed to the sea, and it is full of continental deposits which contribute notably to the flexure of the lithosphere. In Middle Miocene times, important erosion by the Ebro river network takes place and these sediments are transported to the Mediterranean (indicated by dashed arrows), which has just started to open in this region (Late Oligocene). **(c)** Present day: topographic map showing various processes: long-wavelength processes such as the flexure of the lithosphere and sediment erosion; and short-wavelength ones such as Neogene–Quaternary volcanism, or normal faulting and associated grabens in the Catalan Coastal Ranges related to the stretching phase in the Valencia Trough. See text for further explanation.

Furthermore, the erosional unloading of the Catalan Coastal Ranges during Late Miocene and Pliocene times contributed to their uplift, which also affected the configuration of the Ebro Basin, although the relevance and duration of this is not well constrained.

During the Late Oligocene to Middle Miocene, the Valencia Trough underwent important syn-rift subsidence that was accompanied by the accumulation of basal clastics, followed by the deposition of the marine shale and carbonate sequence of the Alcanar group that, at the end of crustal extension, filled in the rift topography (Clavell & Berástegui 1991). At the same time, the Catalan Coastal Ranges underwent a first phase of uplift (Roca & Guimerà 1992; Roca, 2000). From Langhian times onwards, the evolution of the Valencia Trough was characterized by post-rift thermal subsidence and the absence of significant tectonic deformation (Negredo *et al*. 1999). From the Serravallian onwards, the terrigenous shelf-slope complex related to the Ebro sediment supply prograded into the Valencia Trough and resulted in the Serravalian–Tortonian Castellón Group and the Plio–Pleistocene Ebro Group, which

are separated by the deeply incised Messinian unconformity (Clavell & Berástegui 1991; Roca & Desegaulx 1992). During the Messinian, low-standing sea level, large volumes of the Castellón Group were eroded and re-deposited in the deeper parts of the West Mediterranean Basin. Therefore, a realistic material balance between sediments eroded from the Ebro Basin and the Catalan Coastal Ranges and sediments deposited in the Valencia Trough is difficult to establish.

Finally, the occurrence of Late Miocene to Recent volcanism in the eastern Pyrenees, northeastern Ebro Basin and the Valencia Trough (Figs 3 and 5b) must be emphasized. This magmatic activity is related to the rifting transfer zone between the Valencia Trough and Cerdanya to the Rhône–Rhine rift in the north (onshore corresponds to La Garrotxa region and the associated NW–SE-striking fault system in Fig. 5b; Saula *et al.* 1994) and to the overall extensional evolution of the Valencia Trough in the south (Columbretes Islands, Martí *et al.* 1992). This activity distorted the properties of the lithosphere (Lewis *et al.* 2000).

In the studied region, present seismo-tectonic activity is low to moderate (Olivera *et al.* 1992; Masana 1994), except for the Pyrenees (Souriau & Pauchet 1998).

During Late Oligocene to Recent evolution of the Ebro Basin and the Valencia Trough, we observe a combination of long-wavelength features (loading and unloading of the Ebro Basin) and short-wavelength ones (rift-related normal faulting on the Catalan Coastal Ranges and associated grabens; volcanic activity) (Figs 2 and 3).

3 CONSTRAINTS FROM SUBSIDENCE ANALYSIS

In order to obtain an insight into the actual state of load compensation in NE Iberia, we carry out a subsidence analysis by backstripping wells. Such analyses (Steckler & Watts 1978) permit us to quantify the local isostatic component of basin subsidence related to the sediment infill of the available accommodation space. The remaining, tectonic subsidence must be explained in terms of other processes, such as local lithospheric deformation, mantle-derived subsidence/uplift, or may indicate that flexural isostasy is not negligible in the studied basin (e.g. Van Wees *et al.* 1996).

In our analysis, we decompact sediment packages assuming local isostasy, following the procedure of Sclater & Christie (1980). For the sake of simplicity, we make a distinction only between marine and continental series, assuming average lithological properties. Thus, our analysis provides an estimate of the general trend, and not accurate specific values.

The database of our subsidence analysis consists of 43 wells that reach the base of the Tertiary sediments (here considered as the top of the basement) (Lanaja 1987; see Fig. 1 for location). First, we refer the top of the well records to the zero reference level, preserving the observed sediment thicknesses. Following back stripping of these wells, we calculate the *air-loaded* configuration of the top basement surface assuming local isostasy (Fig. 4a). Finally, we correct for the observed topography (elevation of the well location above sea level) by subtracting the air-loaded basement from the topography, giving the so-called *residual surface* (*residual surface* = |*topography*| − |*air-loaded*|). If the sediment infill (topography-corrected) is locally isostatically compensated, this residual surface should be zero. Positive values of the residual surface

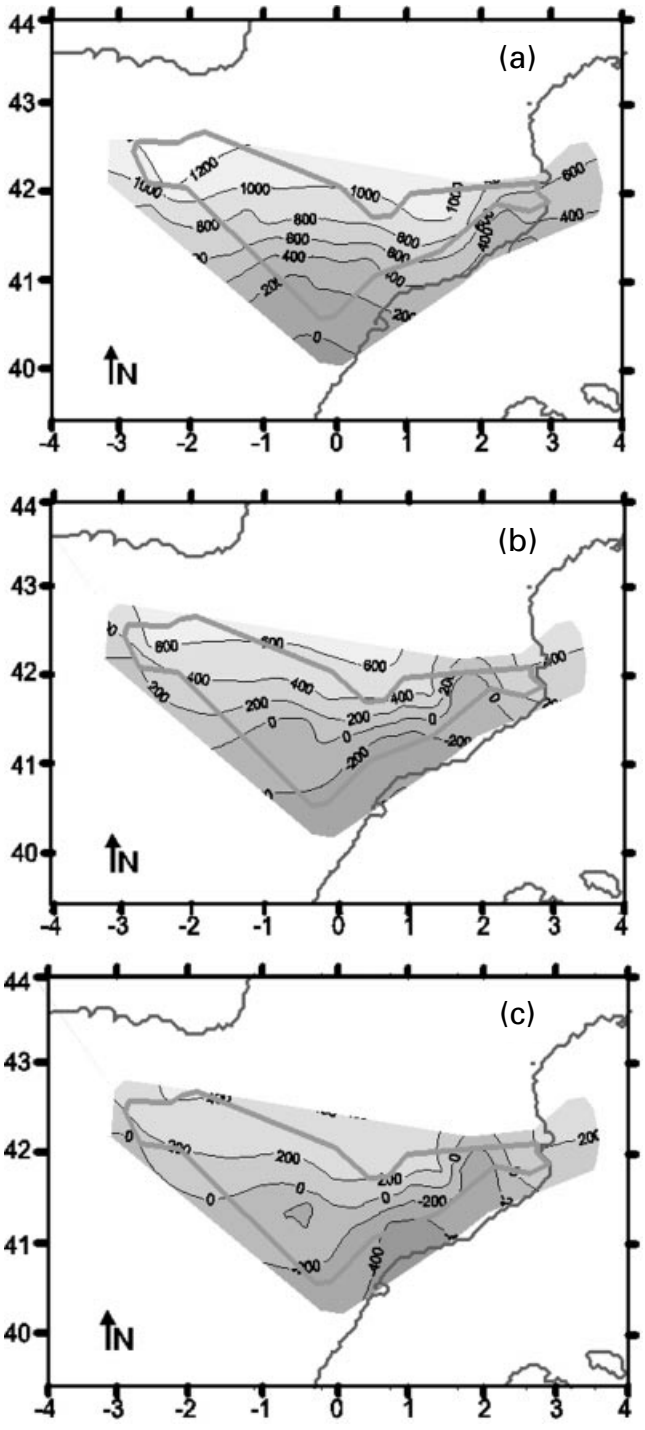

Figure 4. Contour maps of subsidence values derived from well data (Lanaja 1987). The contour interval is 200 m. The residual surface (RS) is defined as follows: *residual surface = air-loaded subsidence − topography*. Zero RS values imply that the sediment infill (topography-corrected) is locally isostatically compensated, positive RS values imply that an extra force is pulling the plate downwards, and negative values imply that **a** force is pushing it upwards. (a) Air-loaded (i.e. resulting from the back-stripping, without topographic correction); **(b)** residual with compaction; **(c)** residual without compaction (constant sediment density).

mean that an extra force, not related to the sediment loading, pulls the plate downwards, whereas negative values are indicative of a force that is pushing it upwards. The residual surfaces we obtained are plotted in Figs 4(b) and (c).

The general trend of northward-increasing values indicates the presence of a lithospheric-scale load that is deflecting the plate downwards, suggesting that the lithosphere compensates for it in a flexural mode. The ultimate cause of this trend is probably related to the Pyrenean orogenic wedge. We do not find any evidence supporting an alternative explanation of this result in terms of lithospheric deformation mechanisms, such as extension and/or asthenospheric upwelling, at least on a regional scale.

Negative and low residual surface values are apparent along the eastern and southern margins of the basin (Fig. 4b). They might be explained as a consequence of tectonic uplift induced by crustal stretching during the development of the Valencia Trough.

We also calculate the subsidence due to local isostatic compensation of sediment fill (topography-corrected) adopting zero compaction for sediments, in order to discern whether or not this parameter has a significant effect on the basin. The resulting residual surface (Fig. 4c) shows lower (absolute) subsidence values and lower gradients. Thus, in the more realistic case in which compaction of the sediments is included (Fig. 4b), additional loads, other than sediment fill (topography-corrected), are required to obtain a good match to the observed basement deflection.

These simple isostasy analyses suggest that the observed subsidence in the Ebro Basin is not caused solely by means of local isostasy with constant sediment density. A regional (flexural) mode of compensation appears to be more applicable in the specific case of the Ebro Basin and its surroundings, maybe with the exception of the southern central Ebro Basin. In this sense, our approach differs from some previous works which assumed local isostasy (Zeyen & Fernàndez 1994; Vergés *et al.* 1998).

Hence, in the Ebro Basin region a 3-D analysis will be applied, including a regional flexure algorithm with sediment compaction correction. In respect of the latter, our approach contrasts noticeably with previous models (Desegaulx & Moretti 1988; Zoetemeijer *et al.* 1990).

4 FLEXURAL MODEL DESCRIPTION AND METHODOLOGY

4.1 Flexural model description

The model used in this study is based on a numerical solution of the 3-D thin elastic plate equation (considering the calculated deflection itself as the third dimension; Van Wees & Cloetingh 1994). It can incorporate loads at the nodes, subsidence due to stretching, sediment compaction correction, and lateral variations in effective elastic thickness (T_e) and depth of necking (z_n). This model has been tested by analytical solutions (Van Wees & Cloetingh 1994) and successfully applied to real cases (Van Wees & Cloetingh 1994, 1996; Van Wees *et al.* 1996).

Thus we consider that the lithosphere behaves as an elastic plate, the thickness of which is the so-called *effective elastic thickness* (T_e). T_e is a measure of the rigidity (D) of the plate. For a plate with Poisson's ratio v, and Young's modulus E, D and T_e are related as follows:

$$D = ET_e^3/[12(1-v^2)]\,. \tag{1}$$

The relation between T_e and the strength of the lithosphere is not so simple (Burov & Diament 1995), although, generally speaking, high values of T_e are associated with strong (normally cold and old) lithosphere, whereas low values are associated with weak (usually warm and young) lithosphere. Although this norm holds for oceanic lithosphere, there are some deviations from the rule for continental lithosphere (Watts 1992), for example due to the presence of horizontal stress fields (Cloetingh & Burov 1996). Nevertheless, Burov & Diament (1995) suggest a method to derive the T_e of a non-purely elastic lithosphere from yield strength envelopes. In Section 5.3 we discuss this subject further.

In our model, the top of the elastic plate corresponds to the top of the basement; that is, the base of Tertiary sediments in the Ebro Basin (since we study the period of foreland sedimentation in the Ebro Basin and syn- and post-rift sedimentation in the Valencia Trough). Hence the subcropping Mesozoic sediments in the Ebro Basin are considered as basement for the flexural calculations, although they are assigned sediment densities in the surrounding outcropping areas (e.g. Iberian Range, southern Pyrenees and Catalan Coastal Ranges).

The initial (pre-orogenic) configuration of the model is an undeformed, horizontal plate with neither topography nor bathymetry. Thus the model ignores the Mesozoic Pyrenean rift structure, and the associated subsidence at those times in the present location of the Pyrenees (Puigdefàbregas & Souquet 1986).

In our approach, no in-plane horizontal stresses are applied. The effect of such stresses would be to produce vertical movements, leading to a deepening of the foreland in the vicinity of mountain belts and uplift on the forebulge (Cloetingh *et al.* 1985). However, the effects of horizontal forces on the bending behaviour of an undeformed strong elastic plate are modest, of the order of a few hundred metres (Turcotte & Schubert 1982; Burov & Diament 1995). The incorporation of horizontal stresses is necessary to study rapid and specific phases of subsidence (uplift), but in the context of our modelling approach they are a second-order effect. For this reason, and because the maximum horizontal present-day stress orientations in the study area are not uniform (Delouis *et al.* 1993; Jurado & Müller 1997; Schindler *et al.* 1998; Goula *et al.* 1999), we opted to exclude this parameter at this stage of our modelling study.

4.2 Modelling methodology

The space created between the observed topography and the deflected basement once the loads are applied is the accommodation space, which is filled in with sediments. We consider that these sediments have the same grain density all over the modelled region, and that they are subjected to compaction. Because this assumption underestimates the density in the zones where the crystalline basement crops out (i.e. no or negligible porosity in the rock; see location in Fig. 5b), we add a differential load (Δq) to compensate it (the *additional load* in Fig. 5a). The value of this load is

$$\Delta q = -gw(\rho_{\text{crust}} - \rho_{\text{sed}})\,, \tag{2}$$

where $g = 9.8$ m s^{-2} is the gravitational acceleration, w the distance from the surface of the observed topography to the top of the deflected plate, and ($\rho_{\text{crust}} - \rho_{\text{sed}}$) the difference between the crustal and sediment densities (see Table 1).

We set the distance between nodes to 5 km, which implies a high bandpass filter that enhances the most significant features

Table 1. Model parameters.

Magnitude	Value	Reference
Initial crustal thickness	32 km	(1)
Initial lithospheric thickness	100 km	(2)
Sediment grain density	2650 kg m^{-3}	(3)
Crustal density	2800 kg m^{-3}	(3)
Lithospheric mantle density	3300 kg m^{-3}	(3)
Water density	1000 kg m^{-3}	(3)
Surface porosity	5×10^{-1}	(4)
Depth porosity relation constant	5×10^{-10} m^{-1}	(4)
Young's modulus	7×10^{10} N m^{-2}	(3)
Poisson's ratio	0.25	(3)
Top asthenosphere temperature	1330 °C	(5)
Thermal diffusivity	7.8×10^{-7} m^{-2} s^{-1}	(5)
Thermal expansion coefficient	3.4×10^{-5} °C	(5)

(1) Banda (1988); (2) Pino & Helmberger (1997); (3) Turcotte & Schubert (1982); (4) Sclater & Christie (1980); (5) Van Wees *et al.* (1996).

at a large scale. Since the seismic lines (ECORS Pyrenees Team 1988; Berástegui *et al.* 1993) clearly show that the lithosphere beneath the Pyrenees is not continuous because the Iberian plate is thrusted under the European plate, we choose a broken plate model to reproduce the structure of this area. We tested this hypothesis with our model by setting the T_e value to zero for the European lithosphere and obtained satisfactory results. Therefore, we use for Iberia an elastic plate with a free boundary located beneath the Pyrenees (Figs 2 and 5b).

We initially proceed by applying different loads to the plate and calculating its deflection. The *calculated deflection* (*c*) will be compared with the *well interpolated surface* (Fig. 6), which is the actual geometry of the top basement surface that results from the interpolation of data points collected from wells and cross-sections (Cámara & Klimowitz 1985; Lanaja 1987; Clavell *et al.* 1988; Berástegui *et al.* 1993; Vergés 1993; Teixell 1996; Muñoz-Jiménez & Casas-Sainz 1997; Vergés *et al.* 1998; Sánchez *et al.* 1999), once the *topographic correction* (*z*) has

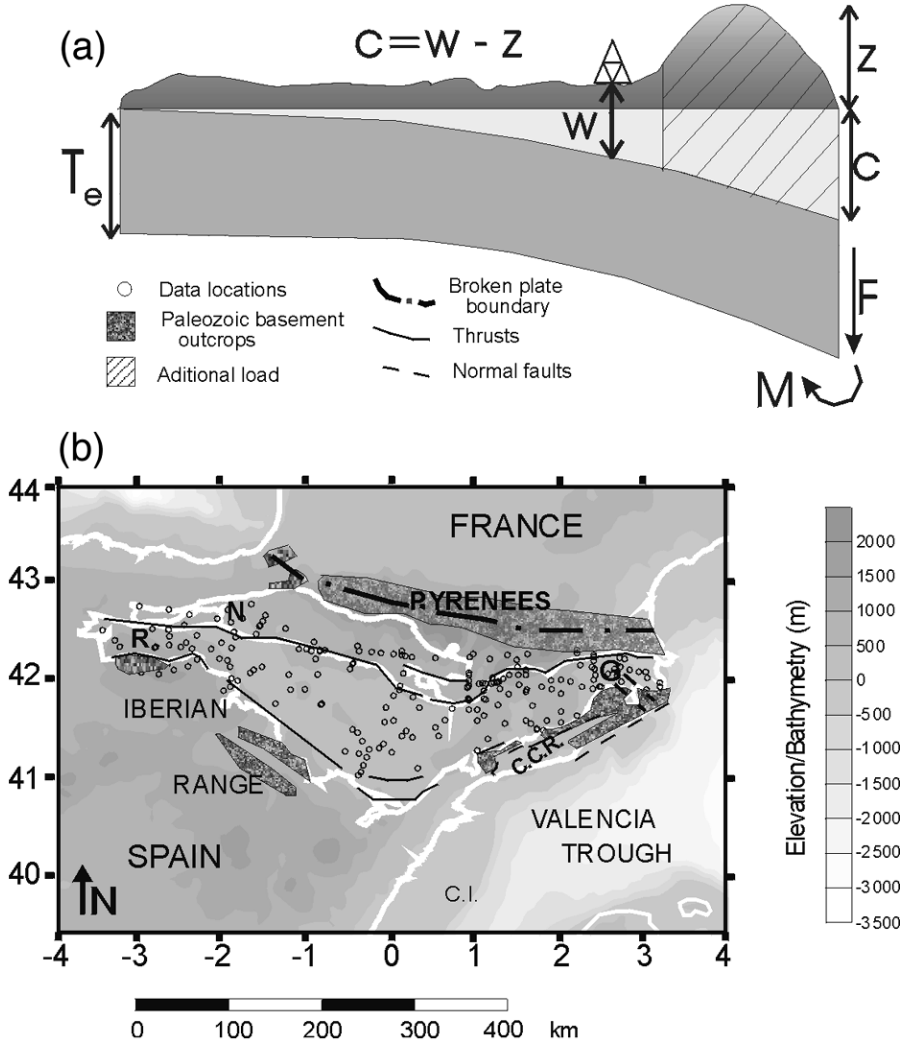

Figure 5. **(a)** Schematic diagram showing the main modelling features. The plate of thickness T_e flexes due to tectonic/topographic and subsurface (*M*, *F*) loads applied at the free boundary of the plate, creating sediment accumulation space. Topographic (*z*) and well (*w*) data are used to constrain the calculated deflection *c*. When equality ($c = w - z$) holds, the parameters used in the calculated deflection surface *c* are satisfactory. z = elevation; c = calculated deflection; w = well-interpolated surface (Fig. 6); M = bending moment; F = shear forces at the broken, free plate boundary; T_e = effective elastic thickness. **(b)** Morpho-tectonic map of NE Iberia, highlighting the most important features pertinent to our modelling (from Riba *et al.* 1983; Losantos *et al.* 1989) and showing data locations. Only main faults concerning this work are depicted. C.I.: Columbretes Islands; C.C.R.: Catalan Coastal Ranges; G: La Garrotxa; N: Navarra; R: La Rioja.

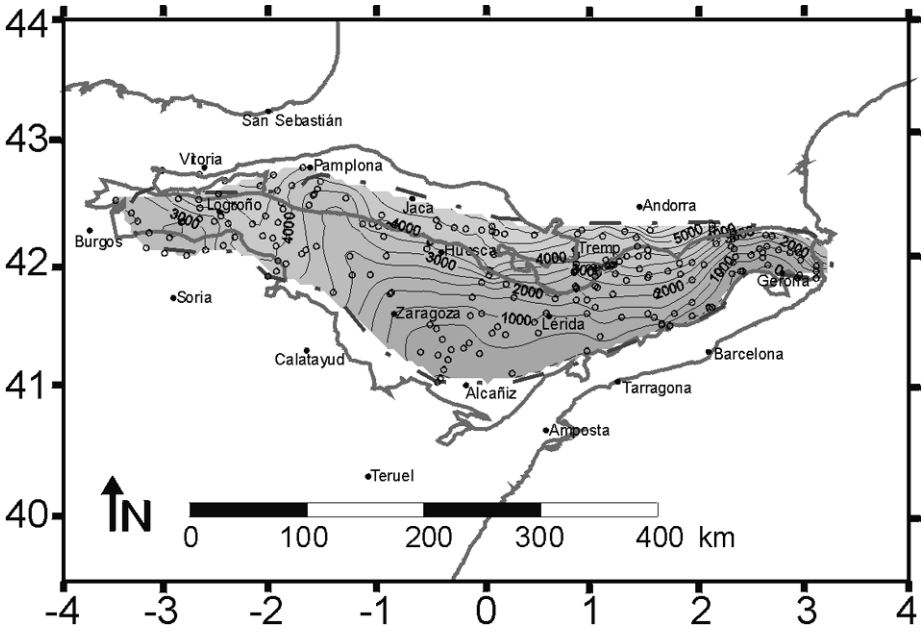

Figure 6. Well-interpolated surface, or depth contour map of top basement (base of the Tertiary) derived from well data (Lanaja 1987) and seismic/structural cross-sections (Cámara & Klimowitz 1985; Clavell *et al.* 1988; Berástegui *et al.* 1993; Vergés 1993; Teixell 1996; Muñoz-Jiménez & Casas-Sainz 1997; Vergés *et al.* 1998; Sánchez *et al.* 1999). Notice double vergence of the flexural basement in the southern Ebro Basin and in La Rioja (western margin). The map is blanked in those areas in which (1) the top basement is deformed by basement-involved thrusts (southern region) and therefore cannot be considered as flexural basement; and (2) an adequate database is lacking (southern and western boundaries). Thus, modelling results in these blanked areas should be taken with caution. For the shake of clarity, a *validity boundary* (dot-dashed line) which separates blanked and non-blanked areas is depicted in the subsequent figures. Contour lines to depth of basement are at intervals of 500 m.

been applied (Fig. 5a). Mathematically this is formulated as

$$d = c - (z - w)\,, \tag{3}$$

where d is the *deviation* or the difference between the two surfaces. When these two surfaces coincide, or in other words when the deviation d is zero, a perfect fit is achieved. Obviously, this approach only works onshore. For offshore areas, the bathymetry has to be considered with the proper density modification (ρ_{water} instead of ρ_{sed}). Taking into account the uncertainties in well data and model parameters, we consider that a deviation of less than 1000 m provides a satisfactory result. Values for parameters used in the model are listed in Table 1.

The Neogene extensional event in the Valencia Trough is also incorporated in our model. The stretching model is based on that of Royden & Keen (1980), which is a variation of the model of McKenzie (1978), by taking different stretching factors for the lithospheric mantle (β_{m}) and the crust (β_{c}). Our model also includes the *level of necking* (z_{n}), which is defined as the level that would remain horizontal during extension in the absence of isostatic forces. Thus, this parameter controls the flexural response of the lithosphere during extension (Braun & Beaumont 1989; Kooi *et al.* 1992).

We ran the model with these loads to find the suitable parameter values and analyse the validity of our hypotheses. We repeated a trial-and-error sequence, changing the initial parameters or the set of loads, until we obtained a good fit. Results of our study are presented in the next section.

5 RESULTS AND DISCUSSION

The relative importance of the individual entities loading the elastic plate, as well as their spatial extents, are discussed below. We give both qualitative and quantitative estimates of the parameters involved in the modelling, and reveal the limitations of our study. A flexural model with variable T_{e} and vertical forces at the free boundary of the (broken) plate yields a satisfactory result.

5.1 Topographic loads

The first inference from the flexural analysis of the present-day situation is the differentiation of two domains of flexural lithospheric response, namely the Ebro Basin and the Valencia Trough domains. The domains interfere in the Catalan Coastal Ranges and the eastern part of the Ebro Basin.

Topographic loading effects exerted on the Ebro Basin are mainly related to the Pyrenees and the Iberian Range; the Catalan Coastal Ranges have a minor effect on the basement deflection of the Ebro Basin, influencing only its eastern margin. Thus, the bending of the plate caused by the topographic loads is directed approximately SSW–NNE. This result is partly due to the nature of our analysis. By using a large-scale modelling approach we are unable to discern local or short-wavelength features, and thus underestimate the load of the Catalan Coastal Ranges (see also Zeyen & Fernàndez 1994; Waltham *et al.* 2000). A more detailed version of the model may overcome this defect (see Section 5.4). On the other hand, the topographic loading exerted by the Pyrenees and the Iberian Range is much larger than the one exerted by the Catalan Coastal Ranges, which implies that the effects of the former dominate over the effect of the latter.

Initial tests and modelling predictions indicate that low T_{e} values fit better in the southern and western regions than in the northern and eastern parts of the Ebro Basin and southern

Pyrenees (Fig. 7). However, the wavelength of the resulting deflection is not large enough to reproduce the configuration of the basement top, regardless of the selected effective elastic thickness. This means that the topographic load itself is not capable of accounting for the observed deflection.

In the next section, we show that the incorporation of extra loads into the model, such as subsurface loads acting on the free boundary of the broken plate, is essential in order to reproduce the configuration of the top basement with the appropriate wavelength.

5.2 Subsurface loads

The next step in our study is the inclusion of a subcrustal load distributed along the free boundary of the broken plate in order to fit the flexure of the plate. This *line load* (along-strike) represents the cumulative effects of, for example, bending moments, slab pull or buoyancy forces arising from the presence of buried anomalous-density bodies (Sheffels & McNutt 1986; Royden 1993).

The effect of this load along the northern boundary of the plate enhances the SSW–NNE basement deflection trend discussed in Section 5.1, and reproduces satisfactorily the wavelength of the flexed basement.

The values we obtain for the line load that provide the best results are between -1×10^{12} and -3×10^{12} N m^{-1} (minus sign denotes downward-directed), increasing from the western region, where the subduction process is less developed (e.g. Vergés *et al.* 1995), to the central and eastern regions. These values are slightly higher than those obtained by Brunet (1986) and Millán *et al.* (1995).

The origin of this subcrustal load in the Pyrenees is related to down-pulling forces exerted by the cold Iberian plate that underthrusts the European lithosphere (Brunet 1986; Beaumont *et al.* 2000; Puigdefàbregas *et al.* 1992). According to several authors, only Iberian continental lower crust and mantle–lithosphere were involved in the underthrusting process (Chery *et al.* 1991; Muñoz 1992; Beaumont *et al.* 2000; Ledo *et al.* 2000). Recent geophysical studies image this slab down to depths of 80–100 km (Souriau & Granet 1995; Pous *et al.* 1995b; Ledo *et al.* 2000). Simple calculations relating the line load required in our model (-1.5×10^{12} Nm^{-1}) to these geometrical constraints (slab 90 km long and 20–50 km thick, depending on the amount of lithospheric material involved in the process), allow us to infer average density contrasts between the underthrusted body and the surrounding lithospheric material of about $\Delta\rho\approx85$ kg m^{-3} (for a thickness of 20 km) and $\Delta\rho\approx35$ kg m^{-3} (for a thickness of 50 km). Given the continental nature of the underthrusted Iberian lithosphere, simply considering a crustal slab would lead to the existence of an upward-directed buoyancy force. Therefore, the presence of high-density bodies located at upper crustal levels (Torné *et al.* 1989), as well as European mantle elements lying on the Iberian crust (Millán *et al.* 1995), must be taken into account.

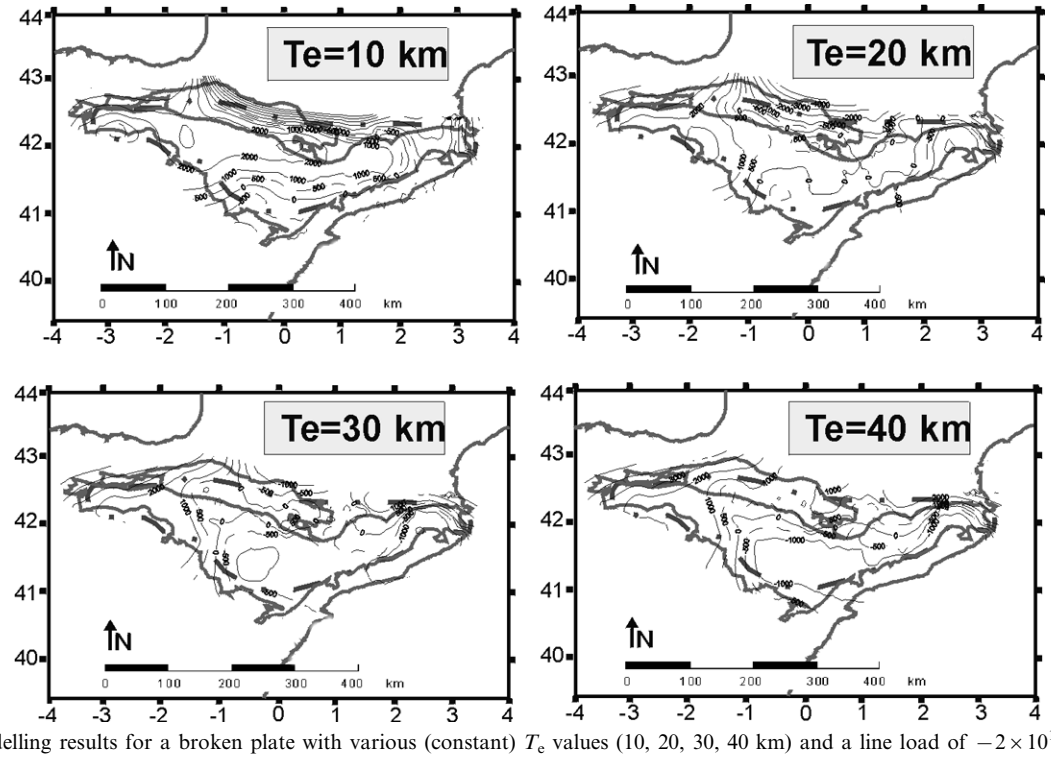

Figure 7. Modelling results for a broken plate with various (constant) T_e values (10, 20, 30, 40 km) and a line load of -2×10^{12} N m^{-1} at the northern edge. Rifting in the Valencia Trough is neglected. The deviation d is represented [eq. (3): $d=c-(z-w)$, where z=elevation (positive) or bathymetry (negative), c=calculated deflection (negative below reference level), and w=well-interpolated surface non-topography-corrected (positive)]. Positive d values indicate a defect of calculated load, and negative d values indicate an excess of calculated load, both with respect to the load required to match the observations perfectly. A zero value of d means an exact match between observations and calculations. The best fit is obtained for T_e values increasing from south ($\approx$10 km) to north ($\approx$30 km) of the Ebro Basin. The dot-dashed line indicates the validity boundary for the observed flexural basement (see legend for Fig. 6).

Furthermore, we note that lower crustal material transforms into eclogite at large depths (>70 km), which significantly increases the mean density and eventually reinforces the downward force (see Dewey *et al.* 1993; Bousquet *et al.* 1997). Such major density transformations within the 'subducted continental slab', in conjunction with rheological changes, must interact in order to reach inferred density contrast. For a more process-based approach, the reader is referred to Chery *et al.* (1991), who carried out a thermomechanical modelling analysis taking into account density variations and various rheologies for the lithosphere.

Once the line load is fixed in our model, we continue by estimating a reasonable value for T_e. For almost the whole Ebro Basin area, relatively high values of T_e ($T_e \approx 20$ km) are derived (Fig. 7), although it is observed that a spatial variation in T_e values is necessary. For instance, we reach the best fit in the westernmost part of the basin for values of T_e between 5 and 10 km, whilst for the central and eastern basin areas and external parts of the Pyrenees, higher values (20–30 km) are required. A trend of increasing values from the central south Ebro Basin to the north Ebro Basin and southern Pyrenees is observed as well. This T_e can be translated into flexural rigidity (eq. 1) giving a value of $D \approx 5 \times 10^{22}$ N m (for $T_e = 20$ km). This high rigidity means that the lithosphere in the Ebro Basin area is relatively strong. These values are in agreement with previous model results for the northern part of the basin (Desegaulx *et al.* 1990; Zoetemeijer *et al.* 1990; and roughly with Millán *et al.* 1995), although the results for the Pyrenees are more controversial. While some authors support low rigidity values in the Pyrenees (Brunet 1986; Millán *et al.* 1995; Beaumont *et al.* 2000), others find high rigidities (Desegaulx *et al.* 1990; Zoetemeijer *et al.* 1990), in accordance with our results.

The decrease in rigidity towards the southwestern basin margin (Fig. 7) could be associated with zones of crustal weakness resulting from several stages of extensional and compressional deformation along the Iberian Range, including the reactivation and inversion of main faults during Cenozoic inversion movements (Salas & Casas 1993; Van Wees & Stephenson 1995). Furthermore, the presence of thrusts (including blind ones) might account for local discrepancies (Zoetemeijer *et al.* 1990). The same reasoning could be applied to the westernmost part of the basin (La Rioja), where important thrusts bound the basin, which in this region is quite narrow (Muñoz-Jiménez & Casas-Sainz 1997). For the northeastern basin edge (La Garrotxa) the previous considerations do not hold. Here, Neogene to Quaternary volcanism and related fault activity have drastically weakened and thinned the lithosphere (Saula *et al.* 1994; Cabal & Fernàndez 1995). For this reason, low values of T_e are more realistic for this particular zone.

In summary, for the study region, modelling predictions clearly point to a loading mechanism dominated by topographic loads in combination with variations of T_e (increasing from the Iberian Ranges towards the external areas of the Pyrenees) and subsurface loads at the northern plate edge.

Discrepancies with previous models that exclude subsurface loads (Desegaulx & Moretti 1988; Zoetemeijer *et al.* 1990) could be attributed to such causes as (1) the application of higher densities (or density contrasts) in basins, resulting in a larger topographic load which causes regional down-flexing of the lithosphere; and (2) a former lack of deep data constraining the flexural basement deflection beneath the external Pyrenees, leading to the exclusion of those parts of the plate where the basement is significantly deflected. Therefore, the proposed basement geometry was unrealistically flat, and did not require an extra vertical, downward-directed load.

5.3 Spatial variations on effective elastic thickness

Following the inferences of our previous modelling predictions, we include in our modelling lateral variations in T_e in order to improve the results. T_e of continental lithosphere is a function of various interdependent factors, such as rheological parameters, geometry of the lithospheric plate and subsurface loads, including bending moments or forces caused by density contrast. Several studies have addressed these relationships (see, for example, McNutt *et al.* 1988; Burov & Diament 1995; and Section 4). In summary, it can be established that T_e is related to two main observables, namely (1) the curvature of the plate (related to, for example, bending moments, dip of the plate) and (2) the surface heat flow (related to lithospheric thermal age), both in an inverse relation.

Concerning the Ebro Basin domain, our previous modelling investigations predict an increase in T_e from south to north (Fig. 7). However, the curvature is higher in the southern Pyrenees than in the Ebro Basin, with the exception of curvature relative maxima in La Rioja and La Garrotxa (western and northeastern Ebro Basin, respectively). This trend would not be expected from the aforementioned T_e dependence on the plate curvature.

We also analysed the possible relationships between the thermal regime and T_e. As shown in the heat flow map of Iberia (Fernàndez *et al.* 1998), some areas of NE Iberia are characterized by important spatial variations in surface heat flow (see also Cabal & Fernàndez 1995). A general decrease in heat flow values from the Ebro Basin towards the Pyrenees is recognized. Fernàndez *et al.* (1998) interpreted these heat flow lateral changes as related to variations in lithospheric thickness. Likewise, Zoetemeijer *et al.* (1990) correlate this heat flow pattern with lateral changes in lithospheric rigidity and correspondingly T_e (higher T_e in the orogen than in the basin). Interestingly, it thus appears that our data show an inverse correlation between plate curvature and surface heat flow data.

In the Valencia Trough domain, the lithosphere is rather weak as it underwent intense rift-related thinning and heating during Late Oligocene-Early Miocene times. This is reflected by high heat flow values (Fernàndez *et al.* 1998). For this reason, low T_e values are expected in this region, as previously proposed by Watts & Torné (1992) and Janssen *et al.* (1993).

5.4 Stretching in the Valencia Trough

Although this study does not aim to analyse the flexure of the lithosphere in the Valencia Trough, we incorporate this mode of deformation in order to investigate the possible effects of extension in the Valencia Trough on the Ebro Basin.

We find that deflection in the Valencia Trough domain due to the topographic loads discussed above (Section 5.1) turns out to be of secondary importance when extension is considered. The removal of lithospheric material and its substitution by sediments and asthenospheric material with a different density dramatically changes the system of loads. In this case there are two new model parameters that control the dynamics of the lithosphere beneath the Trough: (1) the distribution and amount of lithospheric thinning (i.e. map of stretching factors);

and (2) the depth of the necking level (defined in Section 4). We take the level of necking as a free parameter, although we expect it to be not very shallow, in order to produce the observed rift flank uplift, and not very deep, in order to avoid extremely large values of subsidence (Kooi *et al.* 1992).

The choice of the limits of the areas to which stretching factors are applied is crucial. In general, the closer we choose the boundaries of the thinned area (i.e. $\beta_c = 1$, $\beta_m = 1$) to the centre of the Ebro Basin, the larger the effect on the flexure beneath the Ebro Basin. First, estimates of stretching factor values are taken from the literature: β_c factors, of crustal stretching, derived from seismics by Collier *et al.* (1994) and Roca (2000); and β_m factors, of lithospheric mantle stretching, from flexural 2-D modelling (Watts & Torné 1992) and gravity and geoid modelling (Ayala *et al.* 1996). Although the maps from Collier *et al.* (1994) do not show that lithospheric thinning extends onshore, we set the boundary $\beta_c = 1$ beneath the Catalan Coastal Ranges, according to geological and geophysical data (Roca & Guimerà 1992; Vidal *et al.* 1997). In order to obtain a good fit, these stretching factor values need to be modified, although their distribution pattern (i.e. high values on the axis and gradual decrease towards the Iberian margin) is not altered.

Since the lithosphere of the Valencia Trough was strongly affected by the Late Oligocene–Early Miocene rifting phase and is very thin on its axis, low values of T_e are expected (Watts & Torné 1992; Janssen *et al.* 1993), and local isostasy would be a reasonable assumption for the centre of the basin, but not for its flanks (Negredo *et al.* 1999). In our modelling we set T_e between 0 and 15 km for this region.

To validate parameters applied in our modelling, we expect to find an uplift of the Catalan Coastal Ranges of a few hundred metres, and in the centre of the basin a depth to basement (top of pre-rift sediments) of 4–6 km. However, it must be realized that the rifting model we used (based on Royden & Keen 1980) assumes instantaneous initial stretching and therefore no syn-rift cooling of the basin. Such a model can lead to an overestimate of the total subsidence by about 16–20 per cent (e.g. Jarvis & McKenzie 1980). This could be the case for the Valencia Trough, in which the initial tectonic subsidence phase lasted some 8.5–12 Myr and gave way to thermal subsidence around Late Burdigalian–Langhian times (Watts & Torné 1992; Roca 2000).

We tested several positions for the $\beta_m = 1$ boundary, various thinning factor values and lateral variations of the effective elastic thickness. The results are illustrated in Figs 8, 9 and 10.

Fig. 8 is constructed by setting $\beta_m = \beta_c$ ($= \beta$), and locating the boundary of the unstretched region ($\beta = 1$) beneath the Catalan Coastal Ranges, about 10 km from the coast line. We choose a pattern of T_e variations inferred from our previous modelling predictions. A necking level of 15 km provides the best fit.

Fig. 9 shows a modification of the previous model, by placing the boundary $\beta_m = 1$ within the Ebro Basin, about 60 km from the coast line, in agreement with the modelling predictions of Watts & Torné (1992) and Ayala *et al.* (1996), and retaining the rest of the stretching factors as in Fig. 8. T_e variations are derived in the same way as in the preceding case (Fig. 8). The difference between this model and the previous one is that uplift of the Catalan Coastal Ranges occurs as a result of lithospheric mantle stretching distributed over a broad area including the eastern margin of the Ebro Basin. In this model, the necking depth is lowered to 12 km.

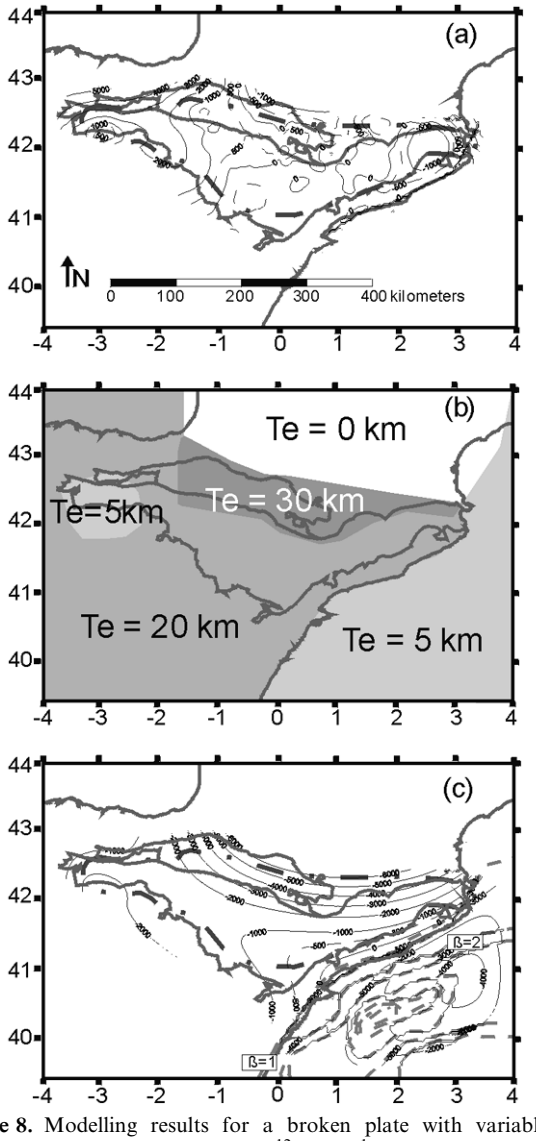

Figure 8. Modelling results for a broken plate with variable T_e values and a line load of -2×10^{12} N m^{-1} at the northern edge, including the effect of the Valencia Trough rifting (stretching factors modified from Collier *et al.* 1994; Roca 2000; and Ayala *et al.* 1996). (a) Deviation plot (see Fig. 7 for explanation). (b) T_e map derived from modelling predictions. (c) Contour lines of calculated deflection c [contour interval is 1000 m (solid line); 500 m contours lines are also depicted (thin-dashed line in the Ebro Basin)]. Contour lines of stretching factors β ($= \beta_m = \beta_c$) are plotted as well (dashed lines in the Valencia Trough area; contour interval is 0.25). Other figure conventions as in Fig. 7.

Fig. 10 is a variation of Fig. 8, obtained by applying T_e variations inferred from the heat flow map of Fernàndez *et al.* (1998) by a simple inverse linear relation. Hence we set a relatively high T_e for the southern Pyrenees (25–35 km), and a lower value to the south (20 km). Finally, following several authors (Watts & Torné 1992; Negredo *et al.* 1999), we adopted for the Valencia Trough a relatively low T_e value (5–15 km). In this case, we used a depth of necking of 15 km.

The distinct scenarios proposed in Figs 8, 9 and 10 yield satisfactory results in the central and eastern parts of the Ebro Basin and in the Valencia Trough. It is, however, more difficult to obtain a good fit in the western part of the study region.

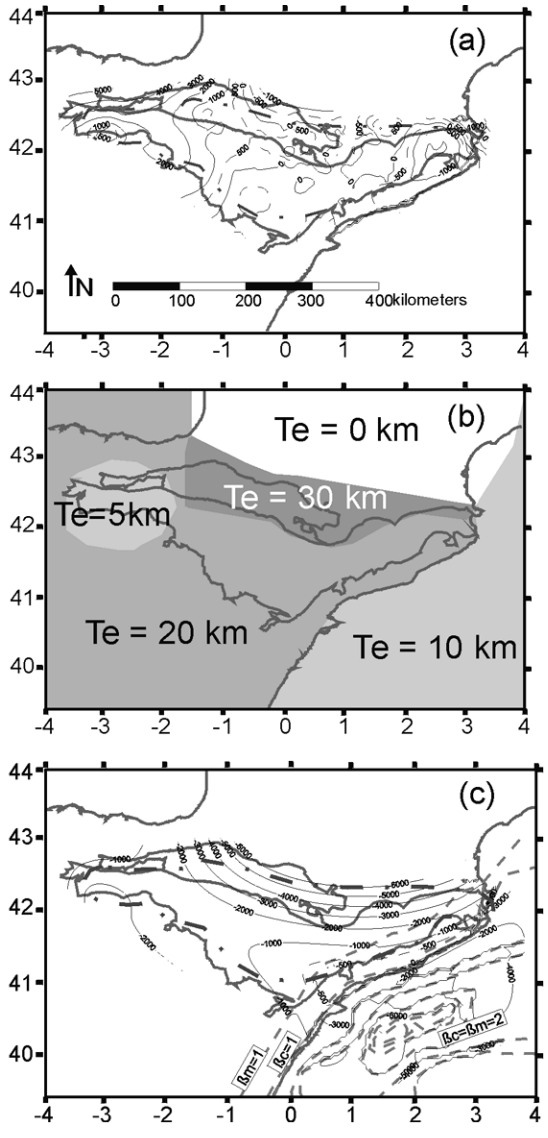

Figure 9. Modelling results for a broken plate with variable T_e and a line load of -2×10^{12} N m^{-1} at the northern edge, including the effect of the Valencia Trough rifting (stretching factors modified from Collier *et al.* 1994; Ayala *et al.* 1996 and Watts & Torné 1992). (a) Deviation plot (see Fig. 7 for explanation). (b) T_e map derived from modelling predictions. (c) Contour lines of calculated deflection. Notice that contours $\beta_m=1$ and $\beta_c=1$ do not coincide. Other figure conventions as in Fig. 8.

Despite differences between the various models presented here and the limitations of our approach, this analysis enabled us to further constrain parameters that should be used in modelling the Valencia Trough.

(1) Necking depths shallower than 10 km lead to negligible uplift in the Iberian flank, and depths greater than 20 km result in exaggerated subsidence of the Valencia Trough. Intermediate necking depths are compatible with the observed uplift/subsidence values. Previous models for the Valencia Trough that include the necking level concept (Janssen *et al.* 1993) indicate intermediate necking levels in the range of 17–33 km. Our modelling predictions reduce this interval to 10–15 km.

(2) T_e variations in the Valencia Trough are of second-order importance when lithospheric stretching is incorporated into the models. In general, low T_e values ($T_e<15$ km) imply greater subsidence of the basin axis and greater flank uplift, affecting a narrow area beyond the hinge zone. The reciprocal situation applies to higher T_e values ($T_e>25$ km).

In the next paragraph we discuss the effects of extension in the Valencia Trough on the Ebro Basin.

5.5 Effects on the Ebro Basin of extensional tectonics in the Valencia Trough

Having constrained the rifting parameters for the Valencia Trough, we proceeded to assess the potential effects of this stretching event on the late evolution of the Ebro Basin.

In this respect, we compared the calculated top basement deflection for a case in which the stretching in the Valencia Trough is included and another in which it is neglected. The difference between the two calculated deflected top basement surfaces (Fig. 11), referred to as the *differential basement deflection* (calculated deflection excluding extension in the Valencia Trough minus calculated deflection including extension in the Valencia Trough), shows that the incorporation of a stretching event in the model provides an extra basement uplift of the Catalan Coastal Ranges of up to 600 m which extends into the centre of the Ebro Basin and decreases towards the northwest.

This has the following important implications for the structure and evolution of the Ebro Basin.

(1) Superimposed on the regional Pyrenees-related SSW–NNE deflection trend (see Section 5.2), the rift-related basement deflection adds a SE–NW tilting component, as observed in the present-day basin configuration (Lewis *et al.* 2000).

(2) This rift-related uplift involved Ebro Basin sedimentary sequences accumulated prior to and during the opening of the Valencia Trough (Late Oligocene times). This new configuration has major repercussions on the erosional pattern of the Ebro Basin. The larger amount of erosion in the eastern Ebro Basin could be related to this uplifting, as well as to the evolution of the drainage network, which was strongly influenced by sea-level changes in the Mediterranean.

(3) Erosional unloading of the Catalan Coastal Ranges and the eastern part of the Ebro Basin caused unflexing of the lithosphere and uplift of these areas. In the Catalan Coastal Ranges, this second phase of uplift, which may still be going on, is superimposed on their earlier rift-related uplift (flank uplift). Moreover, this combination of upward-directed forces could explain the high elevations observed in the eastern part of the Ebro Basin. At the same time, sedimentary material transferred to the Valencia Trough exerts a downward load that contributes to the subsidence of that area. The large extent of the present Ebro Delta and prograding shelf-talud (Fig. 1) gives an idea of the huge amount of material transported.

Comparison of the *differential basement deflection* (Fig. 11) with the present-day distribution of outcropping Palaeocene–Late Eocene sequences (Fig. 3c) reveals a remarkable correspondence, and, together with points (2) and (3), suggests that there is an intimate link between surface and lithospheric-scale processes in this zone. Local deviations in erosional patterns might be explained as resulting from faulting in the Catalan Coastal Ranges and volcanic activity in their northeastern parts.

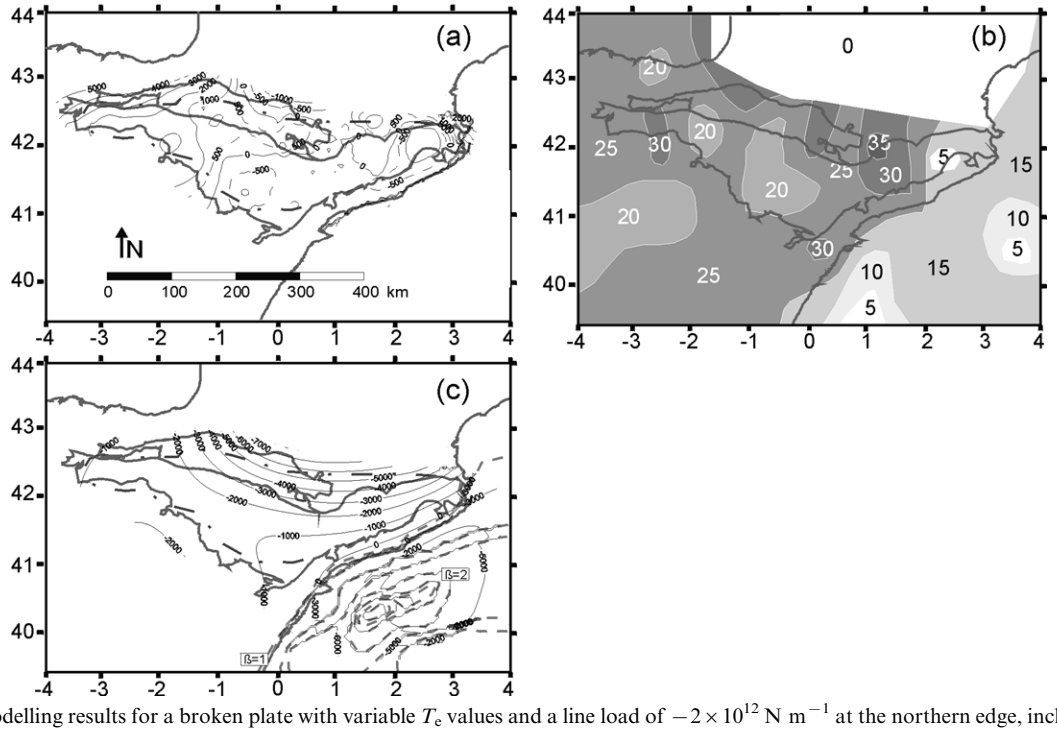

Figure 10. Modelling results for a broken plate with variable T_e values and a line load of -2×10^{12} N m^{-1} at the northern edge, including the effect of the Valencia Trough rifting (stretching factors modified from Collier *et al.* 1994; Ayala *et al.* 1996 and Watts & Torné 1992). (a) Deviation plot (see Fig. 7 for explanation). (b) T_e map derived from the heat flow map of Fernàndez *et al.* (1998) by a simple linear inverse relation ($T_e \propto$–heat flow). (c) Contour lines of calculated deflection. In this case $\beta = \beta_m = \beta_c$. Other figure conventions as in Fig. 8.

Despite the lack of constraints on some of the parameters involved, we attempted to understand how this coupled mechanism works. Assuming that a model without stretching represents the pre-rift stage, and a model including stretching represents the post-rift stage, we obtain an estimate of the amount of material that has been eroded since the beginning of the rifting (Late Oligocene). In this respect, the main uncertainties arise from the lack of knowledge about palaeotopographic

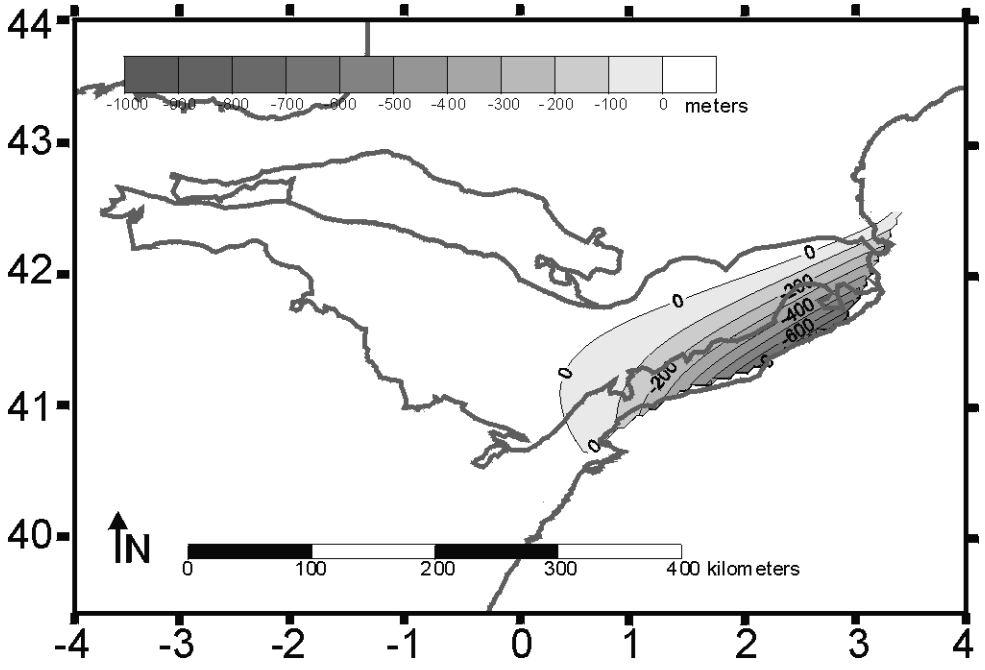

Figure 11. Contour lines of the differential basement deflection; that is, the surface that results from the subtraction of the calculated deflection in the cases in which the stretching in the Valencia Trough is considered and not considered (calculated deflection *excluding* the stretching of the lithosphere in the Valencia Trough—calculated deflection *including* the stretching of the lithosphere in the Valencia Trough). The figure shows that (1) the stretching of the lithosphere in the Valencia Trough affects the eastern Ebro Basin, and (2) the differential uplift predicted as a result of the incorporation of the extensional event in the modelling results in the emplacement of a significant sediment package at elevations above 600 m in the eastern Ebro Basin. Stretching parameters as in Fig. 8. See text for further discussion.

variations during Mio-Pliocene times. If the topography is assumed not to have changed, the contours in Fig. 11 give a direct estimate of the thickness of eroded material. If the topography was higher during the Late Oligocene–Early Miocene, loading would have been greater, the basement would have been flexed down more, and thus more sediment accommodation space would have been created. Hence, the amount of material eroded during Late Oligocene to Present times, as well as the contemporaneous unflexing of the lithosphere, would have been greater. A similar reasoning could be applied to other situations where there is an important interference between tectonic and surface processes.

In summary, although the structure and development of the Ebro Basin were dominated by the emplacement and evolution of orogen-related topographic loads (within and outside the basin) and subcrustal loads, extension in the Valencia Trough had an important effect as well. This feature, which is particularly noticeable when the patterns of sedimentation and erosion are analysed, marks a major difference between the Ebro Basin and many other foreland basins.

6 CONCLUDING REMARKS

Observations on the main morpho-tectonic features of NE Iberia and an analysis of key periods of its geological evolution demanded a 3-D model of this region, the results of which point towards large-scale phenomena that governed the Cenozoic evolution of the lithosphere.

On the basis of isostasy analyses, we showed that a flexural style of isostatic compensation is better able to explain lithospheric-scale phenomena as observed in the study region than local isostasy.

These considerations justified studying the Ebro Basin and surrounding areas in their large-scale tectonic setting. However, it must be kept in mind that the results of such a study are biased by the nature of the method adopted. Thus, the effects of short-wavelength features, such as normal faulting in the Catalan Coastal Ranges associated with the extension in the Valencia Trough domain, thrusting along the boundaries of the Ebro Basin or stacking of Palaeozoic basement units in the Pyrenean axial zone, are difficult to recognize as they compete with other large-wavelength phenomena, such as flexure of the lithosphere due to tectonic loading (Fig. 4). This aspect is evident in the vicinity of the Pyrenean region. There, we are unable to achieve the degree of detail that other smaller-scale studies (i.e. those that focus on finer aspects over smaller areas) do (Beaumont *et al.* 2000; Waltham *et al.* 2000), and we obtain higher rigidity values. Even clearer examples of this are found at the limits of the basin, where local tectonics perturbs general trends (La Rioja and La Garrotxa regions; see Section 5.2.).

A particular effort was made to analyse the significance of short-wavelength features in northeastern Iberia by incorporating lateral variations in effective elastic thickness, and therefore improving the accuracy of our predictions at smaller scales.

Our 3-D large-scale numerical modelling study of thin, elastic plate flexure allows us to draw the following conclusions.

(1) The topographic and tectonic loading effect (within both basins and mountain belts) cannot account for the whole of the observed basement deflections over the entire area addressed by this study, implying the requirement of a subsurface load at the northern, broken boundary of the plate. The basement of the Ebro Basin is deflected in a SSW–NNE direction, with increasing dip towards the Pyrenees, probably partly in response to the load exerted on it by the subducted continental Iberian lithosphere.

(2) The lithosphere in the Ebro Basin is relatively strong, the flexural rigidity being about $D \approx 5 \times 10^{22}$ N m. Values of the effective elastic thickness range around 20 km (generally increasing from south to north). Lower values found along the southwestern basin margin are probably related to weakness zones inherited from Mesozoic rifting and local anomalies produced by thrusting. In general there is a good (inverse) correlation between the heat flow and the effective elastic thickness of the lithosphere.

We have shown that the choice of a purely elastic rheology at this stage is a good first-order approximation, suitable for a large-scale study. To understand the discrepancies between the theoretical and predicted T_e–curvature dependence, and show whether the variations in rigidity can be attributed to flexural yielding, heat flow variations, or a combination of these mechanisms, it will be necessary to incorporate a multilayered rheology using the concept of yield-strength envelopes (Burov & Diament 1995), and to integrate thermal field calculations, faulting and horizontal stresses (e.g. Van Balen *et al.* 1998; Cloetingh *et al.* 1999), which so far has not been implemented in three dimensions.

Our modelling study also includes the effects of the lithospheric extension in the Valencia Trough. According to previous studies and our modelling inferences, we propose two scenarios to explain the observed uplift of the Catalan margin and the subsidence of the Valencia Trough. One possible scenario is that thinning of the lithosphere is restricted to areas seawards of the Catalan Coastal Ranges (Figs 8 and 10). The alternative scenario implies that thinning of the lithosphere extends westwards beneath the Ebro Basin (Fig. 9). Both hypotheses point to an intermediate or low necking level of 10–15 km.

We have shown that rifting of the Valencia Trough affected the Ebro Basin (Fig. 11), controlling both the extent and magnitude of uplift of its eastern parts, thus underlining the requirement to analyse its 3-D setting and conferring on this event a primary role in the late evolution of the Ebro Basin. Rift-related deflection of the lithosphere interferes in the eastern Ebro Basin with the typical flexural foreland basin configuration. Moreover, our results reveal a certain degree of coupling between surface processes (erosional patterns) and tectonic processes (differential uplift induced by the stretching phase in the Valencia Trough). Again local deviations of the erosional pattern close to the Catalan Coastal Ranges can be attributed to low-wavelength upper crustal flexural effects (Zeyen & Fernàndez 1994; Waltham *et al.* 2000), such as normal faulting and Plio-Pleistocene volcanism.

The future development of more detailed 3-D models, including the full interplay between surface and tectonic processes (Burov & Cloetingh 1997), could contribute towards a better understanding of this subject.

ACKNOWLEDGMENTS

This paper is contribution number 20000901 of the Netherlands Research School of Sedimentary Geology (NSG). This work has been partially financed by (1) the Earth and Life Sciences

branch (ALW) of the Netherlands Organization for Scientific Research (NWO); and (2) the CICYT Project PB97–0882-C03 (subprojects 01 and 03), and by the Research Group of Geodynamics and Basin Analysis (99 SGR 64) from Barcelona University.

REFERENCES

Anadón, P., Cabrera, L., Guimerà, J. & Santanach, P., 1985. Paleogene strike-slip deformation and sedimentation along the southeastern margin of the Ebro Basin, in *Strike-Slip Deformation, Basin Formation and Sedimentation,* eds Biddle, K.T. & Christie-Blick, N., *Soc. Economic Paleontologists and Mineralogists Spec. Publ.,* **37,** 303–318.

Anadón, P., Cabrera, L., Colldeforns, B. & Sáez, A., 1989. Los sistemas lacustres del Eoceno superior y Oligoceno del sector oriental de la Cuenca del Ebro, *Acta Geol. Hisp.,* **24,** 205–230.

Ayala, C., Pous, J. & Torné, M., 1996. The lithosphere–astenosphere boundary of the Valencia Trough (western Mediterranean) deduced from 2D geoid and gravity modelling, *Geophys. Res. Lett.,* **23,** 3131–3134.

Banda, E., 1988. Crustal parameters in the Iberian Peninsula, *Phys. Earth planet. Inter.,* **51,** 222–225.

Bartrina, M.T., Cabrera, L., Jurado, M.J., Guimerà, J. & Roca, E., 1992. Evolution of the central Catalan margin of the Valencia trough (western Mediterranean), *Tectonophysics,* **203,** 219–247.

Beaumont, C., Muñoz, J.A., Hamilton, J. & Fullsack, P., 2000. Factors controlling the Alpine Evolution of the Central Pyrenees inferred from a comparison of observations and geodynamical models, *J. geophys. Res.,* **105,** 8121–8145.

Berástegui, X., Losantos, M., Muñoz, J.A. & Puigdefàbregas, C., 1993. Tall geologic del Pirineu central 1: 200000, Servei Geologic de Catalunya, Barcelona.

Bousquet, R., Goffé, B., Henry, P., Le Pichon, X. & Chopin, C., 1997. Kinematic thermal and petrological model of the Central Lepontine metamorphism in the upper crust and eclogitisation of the lower crust, *Tectonophysics,* **273,** 105–127.

Braun, J. & Beaumont, C., 1989. A physical explanation of the relation between flank uplifts and the break-up unconformity at rifted continental margins, *Geology,* **17,** 760–764.

Brunet, M.F., 1986. The influence of the evolution of the Pyrenees on adjacent basins, *Tectonophysics,* **129,** 343–354.

Burov, E. & Cloetingh, S., 1997. Erosion and rift dynamics: new thermomechanical aspects of post-rift evolution of extensional basins, *Earth planet. Sci. Lett.,* **150,** 7–26.

Burov, E. & Diament, M., 1995. The effective elastic thickness (T_e) of continental lithosphere: What does it really mean?, *J. geophys. Res.,* **100,** 3905–3927.

Cabal, J. & Fernàndez, M., 1995. Heat flow and regional uplift at the northeastern border of the Ebro Basin, NE Spain, *Geophys. J. Int.,* **121,** 393–403.

Cámara, P. & Klimowitz, J., 1985. Interpretación geodinámica de la vertiente centro-occidental surpirenaica (cuencas Jaca-Tremp), *Est. Geol.,* **41,** 391–404.

Chery, J., Vilotte, J.P. & Daignières, M., 1991. Thermomechanical evolution of a thinned continental lithosphere under compression: Implications for the Pyrenees, *J. geophys. Res.,* **96,** 4385–4412.

Clavell, E. & Berástegui, X., 1991. Petroleum geology of the Gulf of Valencia, in *Generation, Accumulation and Production of Europe's Hydrocarbons,* pp. 355–368, ed. Spencer, A.M., Oxfrod University Press, Oxford.

Clavell, E., Martínez, A. & Vergés, J., 1988. Morfología del basament del Pirineu oriental: evolucio i relacio amb mantells de corriment, *Acta Geol. Hisp.,* **23,** 129–140.

Cloetingh, S. & Burov, E., 1996. Thermomechanical structure of European continental lithosphere: constraints from rheological profiles and EET estimates, *Geophys. J. Int.,* **124,** 695–723.

Cloetingh, S., McQueen, H. & Lambeck, K., 1985. On a tectonic mechanism for regional sea level variations, *Earth planet. Sci. Lett.,* **75,** 157–166.

Cloetingh, S., Burov, E. & Poliakov. A., 1999. Lithosphere folding: primary response to compression? *Tectonics,* **18,** 1064–1083.

Collier, J.S., Buhl, P., Torné, M. & Watts, A.B., 1994. Moho and lower crustal reflectivity beneath a young rift basin: results from a two-ship, wide aperture seismic reflection experiment in the Valencia Trough (western Mediterranean), *Geophys. J. Int.,* **118,** 159–180.

Coney, P.J., Muñoz, J.A. & McKlay, K.R. & Evenchick, C.A., 1996. Syntectonic burial and post-tectonic exhumation of the Southern Pyrenees foreland fold-thrust belt, *J. geol. Soc. Lond.,* **153,** 9–16.

Delouis, B., Haessler, H., Cisternas, A. & Rivera, L., 1993. Stress tensor determination in France and neighboring regions, *Tectonophysics,* **221,** 413–437.

Desegaulx, P. & Moretti, I., 1988. Subsidence history of the Ebro Basin, *J. Geodyn.,* **10,** 9–24.

Desegaulx, P., Roure, F. & Villien, A., 1990. Structural evolution of the Pyrenees tectonic inheritance and flexural behaviour of the continental crust, *Tectonophysics,* **182,** 211–225.

Desegaulx, P., Kooi, H. & Cloetingh, S., 1991. Consequences of foreland basin development on thinned continental lithosphere: application to the Aquitaine basin (SW France), *Earth planet. Sci. Lett.,* **106,** 106–132.

Dewey, J.F., Ryan, P.D. & Andersen, T.B., 1993. Orogenic uplift and collapse, crustal thickness, fabrics and metamorphic phase changes: the role of eclogites, in *Magmatic Processes and Plate Tectonics,* eds Prichard, H.M., Alabaster, T , Harris, N.B.W. & Neary, C.R., *Geol. Soc. Lond. Spec. Publ.,* **76,** 325–343.

ECORS Pyrenees Team., 1988. The ECORS deep reflection seismic survey across the Pyrenees, *Nature,* **331,** 508–511.

Fernàndez, M., Marzán, I., Correia, A. & Ramalho, E., 1998. Heat flow, heat production, and lithospheric thermal regime in the Iberian Peninsula, *Tectonophysics,* **291,** 29–53.

Fitzgerald, P.G., Muñoz, J.A., Conet, P.J. & Baldwuin, S.L., 1999. Asymmetric exhumation across the Pyrenean orogen: implications for the evolution of a collisional orogen, *Earth planet. Sci. Lett.,* **173,** 157–170.

Goula, X., Olivera, C., Fleta, J., Grellet, B., Lindo, R., Rivera, L.A., Cisternas, A. & Carbon, D., 1999. Present and recent stress regime in the eastern part of the Pyrenees, *Tectonophysics,* **308,** 487–502.

Guimerà, J., 1984. Palaeogene evolution of deformation in the northeastern Iberian Peninsula, *Geol. Mag.,* **121,** 413–420.

Guimerà, J., 1994. Cenozoic evolution of eastern Iberia: Structural data and dynamic model, *Acta Geol. Hisp.,* **29,** 57–66.

Guimerà, J., Salas, R., Vergés, J. & Casas, A., 1996. Extensión mesozoica e inversión compresiva terciaria en la Cadena Ibérica: aportaciones a partir del análisis de un perfil gravimétrico, *Geogaceta,* **7,** 1691–1697.

Jansen, M.E., Torné, M., Cloetingh, S. & Banda, E., 1993. Pliocene uplift of the eastern Iberian margin: Inferences from quantitative modelling of the Valencia Trough, *Earth planet. Sci. Lett.,* **119,** 585–597.

Jarvis, G.T. & McKenzie, D.P., 1980. The development of sedimentary basins with finite extension rates, *Earth planet. Sci., Lett.,* **48,** 42–52.

Jurado, M.J. & Müller, B., 1997. Contemporary tectonic stress in northeastern Iberia. New results from borehole breakout analysis, *Tectonophysics,* **282,** 99–115.

Kooi, H., Cloetingh, S. & Burrus, J., 1992. Lithospheric necking and regional isostasy at extensional basins 1. Subsidence and gravity modeling with application to the Gulf of Lions margin (SE France), *J. geophys. Res.,* **97,** 17 553–17 571.

Lanaja, J.M., 1987. *Contribución de la Exploración Petrolífera Al Conocimiento de la Geología de España,* Publ. IGME, Madrid.

Lawton, T.F., Roca, E. & Guimerà, J., 1999. Kinematic-stratigraphic evolution of a growth syncline and its implications for tectonic development of the proximal foreland basin, southeastern Ebro Basin, Catalunya, Spain, *Geol. Soc. Am. Bull.,* **111,** 412–431.

Ledo, J.J., Ayala, C., Pous, J., Queralt, P., Marcuello, A. & Muñoz, J.A., 2000. New geophysical constraints on the deep structure of the Pyrenees, *Geophys. Res. Lett.,* **27,** 1037–1040.

Lewis, C.J., Vergés, J. & Marzo, M., 2000. High mountains in a zone of extended crust: Insights into the Neogene-Quaternary topographic development of northeastern Iberia, *Tectonics,* **19,** 86–102.

Losantos, M., Aragonès, E., Berástegui, X., Palau, J. & Puidefàbregas, C., 1989. Mapa geològic de Catalunya. Escala 1:250000 Servei Geologic de Catalunya, Barcelona.

McKenzie, D., 1978. Some remarks on the development of sedimentary basins, *Earth planet. Sci. Lett.,* **40,** 25–32.

McNutt, M., Diament, M. & Kogan, M.G., 1988. Variations of elastic plate thickness at continental thrust belts, *J. geophys. Res.,* **93,** 8825–8838.

Martí, J., Mitjavila, J., Roca, E. & Aparicio, A., 1992. Cenozoic magmatism of the Valencia Trough (western Mediterranean): relationship between structural evolution and volcanism, *Tectonophysics,* **203,** 145–165.

Masana, E., 1994. Neotectonic features of the Catalan Coastal Ranges, Northeastern Spain, *Acta Geol. Hisp.,* **29,** 107–121.

Millán, H., Den Bezemer, T., Vergés, J., Muñoz, J.A., Roca, E., Cirés, J., Zoetemeijer, R., Cloetingh, S. & Puigdefàbregas, C., 1995. Palaeo-elevation and effective elastic thickness evolution at mountain ranges: inferences from flexural modelling in the Eastern Pyrenees and Ebro Basin, *Mar. petr. Geol.,* **12,** 917–928.

Muñoz, J.A., 1992. Evolution of a continental collision belt: ECORS-Pyrenees crustal balanced cross-section, in *Thrust Tectonics,* pp. 235–246, ed. McClay, K., Chapman & Hall, London.

Muñoz-Jiménez, A. & Casas-Sainz, A.M., 1997. The Rioja Trough (N Spain): tectosedimentary evolution of a symmetric foreland basin, *Basin Res.,* **9,** 65–85.

Negredo, A.M., Fernàndez, M., Torné, M. & Doglioni, C., 1999. Numerical modeling of simultaneous extension and compression: The Valencia Trough (western Mediterranean), *Tectonics,* **18,** 361–374.

Olivera, C., Susagna, T., Roca, A. & Goula, X., 1992. Seismicity of the Valencia Trough and surrounding areas, *Tectonophysics,* **203,** 99–109.

Pino, N.A. & Helmberger, D.V., 1997. Upper mantle compressional velocity structure beneath the West Mediterranean basin, *J. geophys. Res.,* **102,** 2953–2967.

Pous, J., Muñoz, J.A., Ledo, J.J. & Liesa, M., 1995a. Partial melting of subducted continental lower crust in the Pyrenees, *J. geol. Soc. Lond.,* **152,** 217–220.

Pous, J., Ledo, J., Marcuello, A. & Daignières, M., 1995b. Electrical resistivity model of the crust and upper mantle from a magneto-telluric survey through the central Pyrenees, *Geophys. J. Int.,* **121,** 750–762.

Puigdefàbregas, C. & Souquet, P., 1986. Tecto-sedimentary cycles and depositional sequences of the Mesozoic and Tertiary from the Pyrenees, *Tectonophysics,* **129,** 173–203.

Puigdefàbregas, C., Muñoz, J.A. & Marzo, M., 1986. Thrust belt development in the eastern Pyrenees and related depositional sequences in the southern foreland basin, in *Foreland Basins,* eds Allen, P.A. & Homewood, P., *Spec. Publ. Int. Ass. Sediment.,* **8,** 229–246.

Puigdefàbregas, C., Muñoz, J.A. & Vergés, J., 1992. Thrusting and foreland basin evolution in the Southern Pyrenees, in *Thrust Tectonics,* pp. 247–243, ed. McClay, K., Chapman & Hall, London.

Riba, O., Reguant Serra, S. & Villena Morales, J., 1983. Ensayo de síntesis estratigráfica y evolutiva de la cuenca terciaria del Ebro, in *Libro Jubilar J.M. Ríos. Geología de España, Madrid, I.G.M.E.,* **II,** 131–159, IGME, Madrid.

Rincón, R., Vilas, L., Arias, C., García Quintana, A., Mas, J.R., Alonso, A. & Meléndez, N., 1983. El Cretácico de las Cordilleras intermedias y borde de la meseta, in *Libro Jubilar J.M. Ríos. Geología de España. Madrid, I.G.M.E.,* **II,** 79–103, IGME, Madrid.

Roca, E., 2000. The Northwest-Mediterranean basin (Valencia Trough, Gulf of Lions and Liguro-Provencal basins): structure and geodynamic evolution, in *Peritethys Memoir, IGCP 369. Peri Tethyan Rift/Wrench Basins and Passive Margins,* eds Ziegler, P.A., Cavazza, W. & Robertson, A.F.H., Museum of Natural History, Paris.

Roca, E. & Desegaulx, P., 1992. Analysis of the geological evolution and vertical movements in the Valencia Trough (western Mediterranean), *Mar. petrol. Geol.,* **9,** 167–185.

Roca, E. & Guimerà, J., 1992. The Neogene structure of the eastern Iberian margin: structural constraints on the crustal evolution of the Valencia Trough (western Mediterranean), *Tectonophysics,* **203,** 203–218.

Roca, E., Sans, M., Cabrera, L. & Marzo, M., 1999. Oligocene to Middle Miocene evolution of the Central Catalan margin (North-western Mediterranean), *Tectonophysics,* **315,** 209–229.

Roest, W.R. & Srivastava, S.P., 1991. Kinematics of the plate boundary between Erassia, Ibveria and Africa in the North Atlantic from Late Cretaceous to the present, *Geology,* **19,** 613–616.

Royden, L., 1993. The tectonic expression slab pull at continental convergent boundaries, *Tectonics,* **12,** 303–325.

Royden, L. & Keen, C.E., 1980. Rifting process and thermal evolution of the continental margin of eastern Canada determined from subsidence curves, *Earth planet. Sci. Lett.,* **51,** 343–361.

Sàbat, F., Roca, E., Muñoz, J.A., Vergés, J., Santanach, P., Sans, M., Masana, E., Estévez, A. & Santisteban, C., 1997. Role of extension and compression in the evolution of the eastern margin of Iberia: the ESCI-Valencia Trough seismic profile, *Rev. Soc. geol. España,* **8,** 431–448.

Salas, R. & Casas, A., 1993. Mesozoic extensional tectonics, stratigraphy and crustal evolution during the Alpine cycle of the eastern Iberian basin, *Tectonophysics,* **228,** 33–55.

Salas, R., Guimerà, J., Mas, R., Martín-Closas, C., Meléndez, A. & Alonso, A., 2000. Evolution of the Mesozoic Central Iberian rift system and it Cenozoic inversion (Iberian Chain), in *Peritethys Memoir, IGCP 369. Peri Tethyan Rift/Wrench Basins and Passive Margins,* eds Ziegler, P.A., Cavazza, W. & Robertson, A.F.H., Museum of Natural History, Paris.

Sánchez, J.A., Coloma, P. & Pérez, A., 1999. Sedimentary processes related to groundwater flows from the Mesozoic Carbonate Aquifer of the Iberian Chain in the Tertiary Ebro Basin, northeast Spain, *Sedim. Geol.,* **129,** 201–213.

Saula, E., Picart, J., Mato, E., Llenas, M., Losantos, M., Berástegui, X. & Agustí, J., 1994. Evolución geodinámica de la fosa del Empordá y las Sierras Transversales, *Acta Geol. Hisp.,* **29,** 55–75.

Schindler, A., Jurado, M.J. & Müller, B., 1998. Stress orientation and tectonic regime in the northwestern Valencia Trough from borehole data, *Tectonophysics,* **300,** 63–78.

Sclater, J.G. & Christie, P.A.F., 1980. Continental stretching: an explanation of the post-Mid-Cretaceous subsidence of the Central North Sea Basin, *J. geophys. Res.,* **85,** 3711–3739.

Sheffels, B. & McNutt, M., 1986. Role of subsurface loads and regional compensation in the isostatic balance of the Transverse Ranges, California: Evidence for intracontinental subduction, *J. geophys. Res.,* **91,** 6419–6431.

Souriau, A. & Granet, M.A., 1995. Tomographic study of the Lithosphere beneath the Pyrenees from local and teleseismic data, *J. geophys. Res.,* **100,** 18 117–18 134.

Souriau, A. & Pauchet, H., 1998. A new synthesis of Pyrenean seismicity and its tectonic implications, *Tectonophysics.,* **290,** 221–244.

Steckler, M.S. & Watts, A.B., 1978. Subsidence of the Atlantic-type continental margin off New York, *Earth planet. Sci. Lett.,* **41,** 1–13.

Teixell, A., 1996. The Ansó transect of the southern Pyrenees: basement and cover thrust geometries, *J. geol. Soc. Lond.,* **153,** 301–310.

Teixell, A., 1998. Crustal structure and orogenic material budget in the west central Pyrenees, *Tectonics,* **17,** 395–406.

Torné, M., De Cabissole, B., Bayer, R., Casas, A., Daignières, M. & Rivero, A., 1989. Gravity constraints on the deep structure of the Pyrenean belt along the ECORS profile, *Tectonophysics,* **165,** 105–116.

Torné, M., Banda, E. & Fernàndez, M., 1996. The Valencia Trough: geological and geophysical constraints on basin formation models, in *Peri-Tethys Memoir 2: Structure and Prospects of Alpine Basins and Forelands,* eds Ziegler, P.A. & Horvath, F., *Mem. Mus. Natn. Hist. Nat.,* **170,** 103–128.

Turcotte, D.L. & Schubert, G., 1982. *Geodynamics, Applications of Continuum Physics to Geological Problems,* John Wiley & Sons, New York.

Van Balen, R.T., Podladchikov, Y.Y. & Cloetingh, S.A.P.L., 1998. A new multilayered model for intraplate stress-induced differential subsidence of faulted lithosphere, applied to rifted basins, *Tectonics,* **17,** 938–954.

Van Wees, J.D. & Cloetingh, S., 1994. A finite-difference technique to incorporate spatial variations in rigidity and planar faults into 3-D models for lithospheric flexure, *Geophys. J. Int.,* **117,** 179–195.

Van Wees, J.D. & Cloetingh, S., 1996. 3D flexure and intraplate compression in the North Sea basin, *Tectonophysics,* **266,** 243–259.

Van Wees, J.D. & Stephenson, R.A., 1995. Quantitative modelling of basin and rheological evolution of the Iberian basin (Central Spain): implications for lithospheric dynamics of intraplate extension and inversion, *Tectonophysics,* **252,** 163–178.

Van Wees, J.D., Cloetingh, S. & de Vicente, G., 1996. The role of pre-existing faults in basin evolution: constraints from 2D finite element and 3D flexure models, in *Modern Developments in Structural Interpretation, Validation and Modelling,* eds Buchanan, P.G. & Nieuwland, D.A., *Geol. Soc. Spec. Publ.,* **99,** 283–296.

Vegas, R. & Banda, E., 1982. Tectonic framework and Alpine evolution of the Iberian Peninsula, *Earth evol. Sci.,* **4,** 320–343.

Vergés, J., 1993. Estudi geologic del vessant sud del Pirineu oriental i central, Evolució cinematica en 3D, *PhD thesis,* University of Barcelona, Barcelona.

Vergés, J. & García-Senz, J., 2000. Mesozoic evolution and Cenozoic inversion of the Pyrenean Basin, in *Peritethys Memoir, IGCP 369. Peri Tethyan Rift/Wrench Basins and Passive Margins,* eds Ziegler, P.A., Cavazza, W. & Robertson, A.F.H., Museum of Natural History, Paris.

Vergés, J., Millán, H., Roca, E., Muñoz, J.A., Marzo, M., Cirés, J., Den Bezemer, T., Zoetemeijer, R. & Cloetingh, S., 1995. Eastern Pyrenees and related foreland basins: pre-, syn- and post-collisional crustal-scale cross-sections, *Mar. petrol. Geol.,* **12,** 903–915.

Vergés, J., Marzo, M., Santaeularia, J., Serra-Kiel, J., Burbank, D.W., Muñoz, J.A. & Giménez-Montsant, J., 1998. Quantified vertical motions and tectonic evolution of the SE Pyrenean foreland basin, in *Cenozoic Foreland Basins of Western Europe,* eds Mascle, A., Puigdefàbregas, C., Luterbacher, H.P. & Fernàndez, M., *Geol. Soc. Spec. Publ.,* **134,** 107–134.

Vidal, N., Gallart, J. & Dañobeitia, J.J., 1997. Contribution of the ESCI-Valencia Trough wide-angle data to a crustal transect in the NE Iberian margin, *Rev. Soc. geol. España,* **8,** 417–429.

Waltham, D., Docherty, C. & Taberner, C., 2000. Decoupled flexure in the South Pyrenean foreland, *J. geophys. Res.,* **105,** 16 329–16 340.

Watts, A.B., 1992. The effective elastic thickness of the lithosphere and the evolution of foreland basins, *Basin Res.,* **4,** 169–178.

Watts, A.B. &. Torné, M., 1992. Subsidence history, crustal structure and thermal evolution of the Valencia Trough: a young extensional basin in the Western Mediterranean, *J. geophys. Res.,* **97,** 20 021–20 041.

Zeyen, H. & Fernàndez, M., 1994. Integrated lithospheric modeling combining thermal, gravity and local isostasy analysis: application to the NE Spanish geotransect, *J. geophys. Res.,* **99,** 18 089–18 102.

Ziegler, P.A., 1988. Evolution of the Arctic-North Atlantic and the Western Tethys, *Am. Assoc. petrol. Geol.,* Mem. 43.

Zoetemeijer, R., Desegaulx, P., Cloetingh, S., Roure F., Moretti, I., 1990. Lithospheric dynamics and tectonic-stratigraphic evolution of the Ebro Basin, *J. geophys. Res.,* **95,** 2701–2711.